From molecules to opto-chips: organic electro-optic materials

Larry R. Dalton,*[ab] William H. Steier,[c] Bruce H. Robinson,[a] Chang Zhang,[b] Albert Ren,[b]
Sean Garner,[c] Antao Chen,[c] Timothy Londergan,[a] Lindsey Irwin,[a] Brenden Carlson,[a]
Leonard Fifield,[a] Gregory Phelan,[a] Clint Kincaid,[a] Joseph Amend[a] and Alex Jen[d]

[a]Department of Chemistry, University of Washington, Seattle, WA 98195–1700, USA
[b]Loker Hydrocarbon Research Institute, University of Southern California, Los Angeles, CA
90089–1661, USA
[c]Department of Electrical Engineering, University of Southern California, Los Angeles, CA
90089–0483, USA
[d]Department of Chemistry, Northeastern University, 360 Huntington Avenue, Boston, MA 02115,
USA

Recent advances in polymeric electro-optic materials and device fabrication techniques have significantly increased the potential for incorporation of these materials and devices into modern high bandwidth (fiber and wireless) telecommunication, information processing, and radar systems. Charge transfer π-electron chromophores characterized by molecular first hyperpolarizability (second order optical non-linearity) values approaching 3000×10^{-30} esu have been synthesized. Elucidation of the role of intermolecular electrostatic interactions in inhibiting the efficient translation of molecular optical non-linearity to macroscopic electro-optic activity has permitted systematic modification of materials to achieve electro-optic coefficients approaching 100 pm V^{-1}. Improvements in the optical loss of polymeric materials at wavelengths of 1.3 and 1.55 µm have been effected. Mode matching of passive transmission and active electro-optic waveguides has been addressed, permitting a dramatic reduction in insertion loss. The putative ability of polymeric electro-optic materials to be efficiently integrated with very large scale integration semiconductor electronic circuitry and with passive optical circuitry has been demonstrated. Several devices of varying degrees of complexity have been fabricated and evaluated to operational frequencies as high as 150 GHz. The operational stability of polymeric devices is very competitive with devices fabricated from lithium niobate and gallium arsenide.

Applications of electro-optic materials: from CATV to gyroscopes

The demand for electro-optic modulators has, to a large extent, been driven by the desire for greater bandwidth, for high capacity local area networks (LANs), for video transmission, for optical detection of radar and phased-array radar, for radiofrequency (and microwave to millimetre wave) distribution, and for ultrafast information processing such as analog-to-digital conversion. Both fiber and wireless communication systems are experiencing increased bandwidth demands; electro-optic modulators can perform numerous discrete bandwidth-dependent functions in these systems effectively improving overall system bandwidth.[1] Fortunately, high bandwidth (*i.e.* >300 GHz) is readily obtained with polymeric electro-optic modulators due to low relative permittivities and relatively frequency(wavelength)-independent refractive indices and relative permittivities (permitting radiofrequency and optical waves to co-propagate significant distances without dephasing). Competing technologies for signal transduction, such as modulated lasers, often suffer from bandwidths defined

by electronic state lifetimes in contrast to polymeric modulators where response times are essentially limited by electronic phase relaxation times (corresponding to a few tens of femtoseconds). Polymeric modulators also avoid energy loss that is normally associated with absorptive processes. Since such modulators operate in regions of high transparency, very little heating results. Light scattering is typically the only optical loss mechanism of consequence.

Of course, bandwidth by itself is not enough to ensure the widescale commercial utilization of polymeric electro-optic modulators. Other crucial material characteristics include the magnitude of electro-optic activity (which translates into drive voltage, V_π, requirements), optical loss, stability (including thermal, mechanical, chemical and photochemical stability), and ease of integration with silica fiber optics and very large scale integration (VLSI) semiconductor electronic circuitry.

Moreover, each application of electro-optic modulators, ranging from cable television (CATV),[1] to backplane interconnects between high-speed parallel processors,[2] to gyroscopes for missile guidance,[3] has different material requirements. Requirements are summarized for several applications in Table 1. It is beyond the scope of this article to discuss in detail the numerous applications that are currently being explored for polymeric electro-optic modulators; however, in the course of it we will illustrate several sophisticated device structures and their associated performance characteristics. Our attention is restricted to polymer electro-optic modulator materials that are being developed for application at the telecommunication wavelengths of 1.3 and 1.55 µm.

Like the silicon diode, electro-optic modulators can be configured to perform a variety of functions from electrical to optical signal transduction, to optical switching, to millimeter wave signal generation, to optical beam steering, to radiofrequency (also microwave and millimeter wave) detection, to phase control, to power splitting, to wavelength division multiplexing (WDM). For each of these applications, electro-optic modulators must compete with established alternative technologies; however, as drive voltage requirements and loss characteristics of modulators improve and as the bandwidth

Table 1 Bandwidth and drive voltage requirements for several applications of electro-optic modulators

Application	Bandwidth	Drive voltage/V
Cable TV, datacom	Lower GHz	5–10
Telecom	Higher GHz	2–3
RF Photonics	Higher GHz	<1

requirements of various applications increase, modulators are more likely to become the technological approach of choice. Hopefully, the ultimate competition to electro-optic modulation will come from all-optical processing based on the Kerr effect. Such all-optical processing depends upon third order, rather than second order, optical non-linearity. The magnitudes of third order optical non-linearities are not adequate at the present time.

Pockell's effect: the macroscopic phenomenon of electro-optic activity

The velocity of light (electromagnetic radiation) in a material is determined by the interaction of the electric field component of light with the charges (electronic and nuclear) of the material. The effect is quantitatively defined by the index of refraction, n, of the material, which is the ratio of the speed of light in a vacuum to that in the material. Consider the application of an electric field to a material of magnitude sufficient to change the charge (*e.g.*, electronic) distribution of the material. This would, in turn, change the velocity of light in the material and the index of refraction of the material. We could then speak of an electric field-dependent index of refraction (or phase shift, called the Pockell effect) of the material: $\Delta\phi = \pi n^3 r V L/\lambda$ and $V_\pi = \lambda h/n^3 r L$ where $\Delta\phi$ is the electric field dependent phase shift of light passing through an electro-optic material, V the applied electric field, h the electrode spacing, n the field-independent index of refraction, r the electro-optic coefficient of the material, L the length of the material (distance over which the electric and optical fields co-propagate and interact *via* the electro-optic material), λ the wavelength of light, and V_π the voltage required to produce a π phase shift.

This property of the material can be used to manipulate light; for example, to produce a controlled phase shift, to switch light at waveguide nodes, and to steer light. Of course, we are immediately faced with two issues: (1) what are some specific device structures that can make effective use of Pockell's effect and (2) how can we find a material where the charge distribution can be dramatically changed by the application of a small electric field (say of one volt magnitude)?

Application of electro-optic materials: simple device structures

In Fig. 1 we show two simple device configurations useful for application of electro-optic materials; namely, signal transduction and optical switching.[4] The top schematic illustrates a Mach Zehnder modulator. The input (I_i) and output (I_o) light for a Mach Zehnder (MZ) device are related by $I_o = I_i \sin[(\phi_{ba} + \Delta\phi)/2]$ where ϕ_{ba} is the phase difference between the arms without application of an electric field and $\Delta\phi = \pi n^3 r_{33} V L/\lambda h$. For a MZ modulator, the drive voltage, V_π, is given by $V_\pi = \lambda h/n^3 r_{33} L$; r_{33} is the component of the electro-optic tensor that lies in the applied electric field direction. The MZ modulator acts to transduce an electric signal onto an optical transmission as an amplitude modulation. If no electric field is applied, the signals that were split apart by the first Y-junction recombine to give the original signal at the second Y-junction. If an electric field of magnitude appropriate to produce a phase shift of π is applied only to one arm of the MZ device, then the signals will cancel at the second Y-junction.

The second device configuration shown in Fig. 1 is that of a directional coupler. A directional coupler acts as a routing switch at a node in an optical network and consists of two side-by-side waveguides separated by a few micrometres. The overlap of the guided waves in the two waveguides couples energy back and forth between the waveguides. When a low
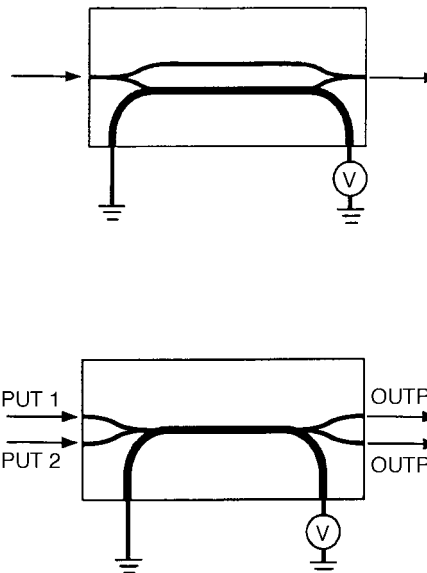

Fig. 1 Schematic representations of Mach Zehnder (upper) and directional coupler (lower) device configurations.

frequency voltage is applied the intensities at the output ports are determined by either modulation of the phase mismatch, $\Delta\beta$, or the coupling coefficient κ. Thus, change of voltage by an amount V_π switches an input signal from one output port to the other. The smallest voltage, required for switching light from one output port to the other, is 1.7 times larger than required for a π phase shift in a MZ modulator. The drive voltage requirement for a directional coupler is thus somewhat more demanding than for a MZ modulator.

Polymeric modulators *versus* lithium niobate modulators

Lithium niobate is currently the dominant material in modern electro-optic modulator technology. It is a crystalline ferroelectric material that has been under development for a number of decades. Commercial modulators (typical cost: $6,500) are available from companies such as United Technologies, Uniphase Telecommunication Products, and Lucent Technologies. These modulators operate to 10 GHz with drive voltages (V_π) in the 5–6 V range. Lithium niobate modulators permit very low insertion loss 3–5 dB (half that of currently available polymeric and GaAs modulators). Unless polymer modulators prove to be much less expensive than those fabricated from LiNbO$_3$, discrete modulators for low frequency applications will likely continue to be fabricated from lithium niobate.

However, polymer electro-optic materials have some significant advantages over crystalline materials. It is applications, which rely on these advantages, which will likely promote the commercialization of polymeric modulators. Thus, although polymers have the potential for lower cost than competing materials, device cost is heavily influenced by packaging and other issues.

We have already alluded to the first advantage of polymeric modulators, namely that of exceptional bandwidth. The bandwidth of modulators derives from the near equality of n(optical) and n(millimetre wave) so that optical and millimetre wave electromagnetic radiation can co-propagate over significant distances without de-phasing. For 100 GHz operation, a polymeric modulator can be 2 cm long while a lithium niobate device is limited to approximately 1 mm. Successful lithium niobate modulators have been demonstrated to 70 GHz employing clever velocity matched structures to increase the interaction length. Even employing simple device structures

(standard stripline), polymeric electro-optic modulators have been operated in the 100–200 GHz range and have been shown to have a 3 dB bandwidth of 361 GHz.[5]

Another advantage of polymeric modulators is the low relative permittivity of polymers relative to ferroelectric lithium niobate. This creates the possibility of positioning several individual high-speed modulators close to one another without causing degrading radiofrequency crosstalk between the modulators. We shall see later that crosstalk between adjacent modulators is down by a factor of at least 50 dB (*i.e.* essentially unmeasurable).[6] This feature leads to the possibility of packaging several modulators in the same module for compact multi-channel optical communication links.

A third advantage of polymer modulators relevant to high density packaging and integration with very large scale integration (VLSI) semiconductor electronics is that polymeric electro-optic materials can be deposited onto and will adhere to many substrates including semiconductor electronics. Also, polymeric modulators can be fabricated on flexible substrates such as Mylar leading to conformal modulator devices, *e.g.* relevant to airborne applications. This compatibility of electro-optic polymers with a variety of materials is a significant first step in the development of opto-chips (integrated opto-electronic chips). Moreover, the processability and temperature stability of polymer materials are compatible with the many steps of full opto-electronic integration. In constrast, only hybrid integration using separate optical and electronic modules connected *via* cables for flip-chip bonding is possible with crystalline lithium niobate. There are well established semiconductor foundries that can produce custom chips to design. The ability to interface with this sophisticated electronic device manufacturing capability is a significant advantage for polymeric materials. We have demonstrated that polymers are indeed ideally suited for the development of sophisticated integrated opto-electronic packages where control, drive, and interface electronics are directly integrated with polymeric modulators.[6]

Yet another advantage of polymeric modulator materials is the ability to integrate active polymer materials into an optical circuit that includes other optical materials.[6] The key technology of this integration involves the ability to fabricate low loss vertical waveguiding structures in polymers. Such structures provide interconnection of multiple layers in optical integration. Low angle vertical shapes can be fabricated by reactive ion etching using either oxygen or carbon tetrafluoride. Slow vertical tapers with heights of several μm and lengths of a millimetre or less can be patterned and etched.[6] This makes it possible to fabricate vertical waveguide bends and vertical waveguide power splitters that are some of the key elements for three dimensional integrated optics. This aspect of polymers also permits minimization of optical loss associated with polymeric electro-optic modulators as light can be directed into the polymer modulator for signal processing and back into the low loss passive waveguide for transmission. Residence time in the more 'lossy' (high optical loss) active waveguide is minimized.

A final advantage of polymeric electro-optic materials is the potential for dramatically lower operating voltages. Drive voltages of less than one volt have already been demonstrated for polymeric modulators compared to five volts (with little or no possibility for dramatic improvement) for lithium niobate modulators. With ever improving chromophore/polymer design, drive voltages of 0.1 (or even less) will most likely be achieved for polymeric materials.

Molecular hyperpolarizability: the microscopic phenomena and structure function relationships

Molecular optical non-linearity (non-linear polarization) can be expressed as a power series expansion in powers of the electric field (arising from electromagnetic fields of various frequencies).[7] Thus, the molecular polarization, p_i, can be written as in eqn. (1)

$$p_i = \alpha_{ij}E_j + \beta_{ijk}E_jE_k + \gamma_{ijkl}E_jE_kE_l + \dots \qquad (1)$$

where α is the linear polarizability, β the first molecular hyperpolarizability and γ the second hyperpolarizability. We shall focus on the second term in this expansion and in particular on the case where E_j is typically a radiofrequency (or microwave or millimetre wave) field and E_k is an optical field (*e.g.* 1.3 or 1.55 μm wavelength). For β to be non-zero, molecules of acentric (dipolar) symmetry are required. An obvious candidate for highly polarizable materials of acentric symmetry is a charge-transfer molecule of the general formula (electron donor)(π-electron bridge)(electron acceptor). Such a molecule is frequently viewed as being characterized by a neutral ground state and a charge-separated excited state. Application of an electric field effects a change in the mixing of these two forms and thus the molecular polarization. The reverse situation of a charge-separated ground state and neutral excited state can also be envisioned; for such a situation, β is negative. It is obvious that the ground state of a real molecule will lie between these two extremes reflecting an admixture of the neutral and charge separated forms. Marder and co-workers[8] have shown that β values vary in a sinusoidal manner with changing admixtures of neutral and charge separated forms. This sinusoidal variation is predicted by a simple two-state quantum mechanical model that explicitly leads to expression (2)

$$\beta = (\mu_{ee} - \mu_{gg})(\mu_{ge})^2/(\Delta E_{ge})^2 \qquad (2)$$

where $(\mu_{ee} - \mu_{gg})$ is the difference between the excited and ground-state dipole moments, μ_{ge} the transition dipole moment (transition matrix element connecting the ground and excited state), and ΔE_{ge} the optical (HOMO − LUMO) bandgap. Each of the three fundamental parameters of eqn. (2) will vary in a predictable way with molecular structure. The dependence of dipole moment upon charge separation is obvious. The bandgap will go to zero as bond length alternation in the π-electron bridge structure goes to zero. A variety of empirical structure/function correlations have been developed to assist the design of chromophores with ever increasing β values. Marder and co-workers[8] have shown how structural modification of chromophores shifts β along the sinusoidal curve of β plotted against bond length alternation of the bridge structure. Other empirical correlations can also be developed. For example, for organic acid acceptors, β can be correlated with the pK_a of the acceptor.[9] Such empirical structure/function relationships complement those developed from more rigorous theoretical treatments.[10]

The structure/function relationships developed by Marder and co-workers[8] and by others have been extremely successful in guiding the development of ever improving β values to currently observed state-of-the-art values of 3000×10^{-30} esu from values of 10×10^{-30} esu for compounds such as methyl 4-nitrophenyl sulfide. In Fig. 2 we illustrate representative examples of such molecules and the variation of molecular optical non-linearity with molecular structure.

Researchers attempting to develop new chromophores for electro-optic applications have tended to focus upon molecular hyperpolarizability. However, for a chromophore to have potential for translation to a polymeric electro-optic material for device fabrication the chromophore must be very robust. Mechanical, thermal, chemical, and photochemical stability are required. As polymeric electro-optic materials must withstand temperatures somewhat above 100 °C for long periods of time and short term excursions (during electrode deposition) to even higher temperatures, thermal stability to temperatures of the order of 250 °C are required for chromophores to be practical for device applications. Since high glass transition
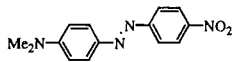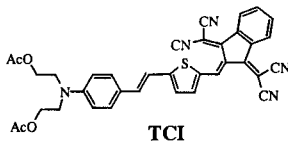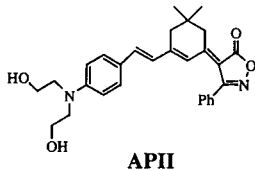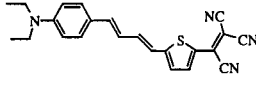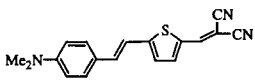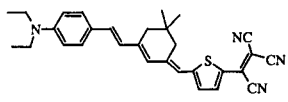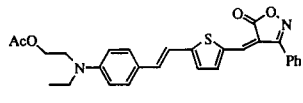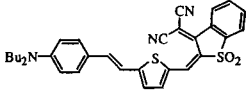
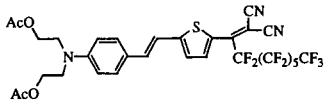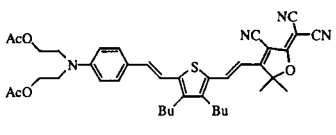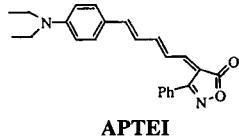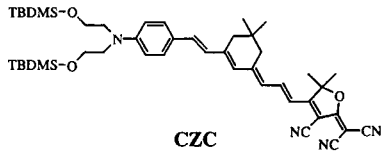| Structure	$\mu\beta/10^{-48}$ esu	Structure	$\mu\beta/10^{-48}$ esu
DR, 30 wt%, $r_{33} = 13$ pm V^{-1}	580	TCI	6100
APII	926		9800
	1300		13000
ISX	2000	SDS	15000
FCN	3300	FTC, 20 wt%, $r_{33} = 55$ pm V^{-1}	18000
APTEI	~4000	CZC	35000

Fig. 2 The variation of the product of dipole moment, μ, and molecular first hyperpolarizability, β, with chromophore structure. This product is, in the absence of intermolecular electrostatic interactions, a chromophore figure of merit for estimating the expected macroscopic electro-optic activity of polymeric materials incorporating various chromophores. TBDMS = *tert*-butyldimethylsilyl.

polymers yield the most thermally stable electro-optic materials, it is desirable for chromophores to exhibit thermal stability to 300 °C or above. In Fig. 3 we illustrate the variation of chromophore decomposition temperature (determined by thermal gravimetric analysis and differential scanning calorimetry), together with molecular optical non-linearity, with chromophore structure.[11] It is clear that good thermal stability and high optical non-linearity are not mutually exclusive. Researchers at IBM have used cyclic voltammetry to define chromophore chemical (electrochemical) stability.[11] For example, replacing alkylamine donor groups with arylamine donors was shown to yield improved chromophore stability.

A few comments regarding the experimental characterization of molecular first hyperpolarizability are appropriate. The two most commonly employed methods of characterizing molecular optical non-linearity are electric field induced second harmonic generation (EFISH)[12] and hyper-Rayleigh scattering (HRS);[13] the former measures $\mu\beta$ while the latter measures β. Caution must be exercised in interpreting HRS data as two photon effects can lead to artificially high β values. Molecular first hyperpolarizability values β depend on wavelength (frequency) so specification of measurement wavelength is important in comparing different compounds. Here $\mu\beta$ values are reported for a measurement wavelength of 1.9 µm. This wavelength is sufficiently removed from the interband electronic

transition as to be a reasonable approximation of the long wavelength (zero frequency) limit. An explicit expression for the frequency dependence of β can be derived from the simple two state model discussed above and is useful for relating measurements at different wavelengths.[14]

Translating hyperpolarizability into macroscopic electro-optic activity

Macroscopic second order optical non-linearity (electro-optic activity and second harmonic generation) can be measured by a variety of techniques including ellipsometry,[15] attenuated total reflection,[16] two slit interference modulation[17] and second harmonic generation.[18] We have recently introduced a modification of the attenuated total reflection method that permits rapid interchange of samples.[19] Electro-optic coefficients can also be determined from the various device configurations discussed in this article.

For macroscopic electro-optic activity to be finite (non-zero), chromophores must exhibit net acentric order, *i.e.* they must be oriented to yield a dipolar chromophore lattice. Such acentric (or non-centrosymmetric) order is most commonly introduced by electric field poling.[20] Other methods of producing acentric chromophore lattices include crystal growth, incor-
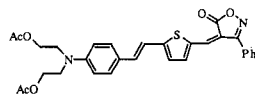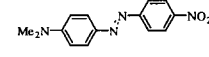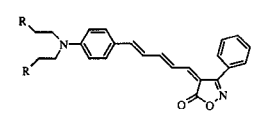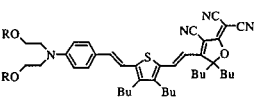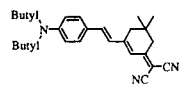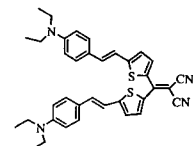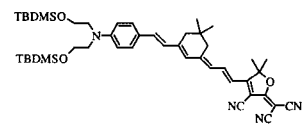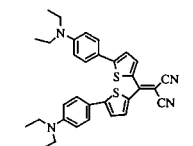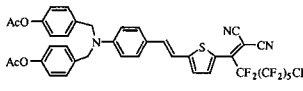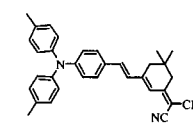
Structure	T_d/°C	$\mu\beta$/10^{-48} esu	Structure	T_d/°C	$\mu\beta$/10^{-48} esu
(chromophore structure)	200	2000	(chromophore structure)	307	580
(chromophore structure)	203	5600	(chromophore structure)	310	18000
(chromophore structure)	268	2520	(chromophore structure)	325	2500
(chromophore structure)	271	35000	(chromophore structure)	354	1300
(chromophore structure)	274	3300	(chromophore structure)	367	2570

poration of chromophores into inclusion compounds, and sequential synthesis methods where chromophore lattices are built up from a substrate surface utilizing layer-by-layer deposition methods.[20] Here, we restrict our consideration to acentric lattices prepared by electric field poling.

Macroscopic optical susceptibility (including non-linearity) can also be expressed as a power series expansion in powers of the applied electric field. An expression for macroscopic polarization, P_i, can be written that is analogous to microscopic polarization expressed in eqn. (1) with α replaced by $\chi^{(1)}$, β by $\chi^{(2)}$, and γ by $\chi^{(3)}$ where $\chi^{(1)}$ is the first order optical susceptibility and $\chi^{(2)}$ and $\chi^{(3)}$ are respectively the second order and third order non-linear optical susceptibilities. For polymeric electro-optic modulator materials, the linear (first order susceptibility) term is comprised of contributions from the non-linear optical chromophore and the host polymer. Note that the host polymer does not contribute to optical non-linearity since it is composed of σ bonded segments and it is the delocalized π-electron structure of the chromophore that dominates optical non-linearity. The contributions of the NLO chromophore to the first and second order non-linear optical susceptibilities can be written as follows: $\chi^{(1)}(c) = Nf_j(\omega) <\alpha_{ij}>$ and $\chi^{(2)}(c) = Nf_i(\omega)f_j(\omega)f_k(0) <\beta_{ijk}>$ where N is the chromophore number density (molecules cm^{-3}), f are local field factors, and $< >$ denotes the average or expectation value of the observable. Explicitly, $<\alpha_{ij}> = <q_{ui}q_{vj}>\alpha_{uv}$ and $<\beta_{ijk}> = <q_{ui}q_{vj}q_{wk}>\beta_{uvw}$, where the q_{ui} are rotation matrix elements relating the molecular (u,v,w) and laboratory (i,j,k) axes. The macroscopic electro-optic coefficient, r_{33}, relevant to poled polymeric materials can be related to β_{zzz} by expression (3)

$$r_{33} = -2\chi^{(2)}_{zzz}/(n_z)^4 = -2N[f_z(\omega)]^2 f_z(0)\beta <\cos^3\theta>/(n_z)^4 \tag{3}$$

where ω is angular frequency and θ is the angle between the poling field direction and the chromophore principal axis.

We have already seen that it is this component of the electro-optic tensor that is relevant to the performance of the MZ modulator shown in Fig. 1.

Obviously, the competition of chromophore/electric poling field interactions, U_1 (which induce acentric order), and thermal randomization events are important in defining the acentric order parameter $<\cos^3\theta>$. A commonly employed approximation in the computation of $<\cos^3\theta>$ is to neglect chromophore–chromophore intermolecular electrostatic interactions. With this approximation, the potential function used in the statistical mechanical computation of order parameter is simply $U_1 = -\mu f_p E_p \cos\theta$ where μ is the chromophore dipole moment, E_p the magnitude of the applied electric poling field and $f_p E_p$ is the effective poling field felt by the chromophore. Note that $f_p E_p = V/h$ where V is the applied poling voltage and h the thickness of the film being poled (or the electrode spacing). Typical poling fields are of the order of one to several hundred volts per μm. In order to understand the various types of local field factors and the various frequency dependences of the above equations it is important to keep in mind that three types of electrical fields are involved in our considerations: a high frequency optical field typically of 1.3 or 1.55 μm wavelength, a low frequency (radiowave to milliwave) field, and the dc poling field. Note that the low frequency and poling fields typically have the same symmetry, i.e., they are applied along what we denote as the z laboratory axis. The order parameter is readily computed following the prescriptions of statistical mechanics applied to Boltzmann particles,[21] eqn. (4)

$$<\cos^3\theta> = L_3(\mu f_p E_p/kT) \tag{4}$$

where L is the Langevin function defined by eqn. (5)

$$L_3(x) = \int \cos^3\theta \cdot \exp(-x\cos\theta) d[\cos\theta]/$$
$$\int \exp(-x\cos\theta) d[\cos\theta] = x/5 = \mu f_p E_p/5kT \tag{5}$$

where $x = \mu f_p E_p / kT$. The above integrals are evaluated between the limits of $\cos\theta = -1$ and $+1$ corresponding to $\theta = 0$ and $180°$. To obtain the above limiting expression we have assumed $\mu f_p E_p < < kT$ and retained only the first term of the power series expansion of x. The local field factors are normally treated, following Onsager,[22] by considering the contribution of the reaction field from the induced dipole moment of a molecule in a cavity to the cavity field. For this treatment the local field factors are given by $f_i = (n_i)^2 [(n_c)^2 + 2]/[2(n_i)^2 + (n_c)^2]$ and $f_p = \varepsilon [(n_c)^2 + 2]/[2\varepsilon + (n_c)^2]$ where n_c represents the index of refraction of a medium composed of molecules with polarizability α packed together with a cavity radius of c. Notice that when $n_c = n_i$ and $(n_c)^2 = \varepsilon$ the Onsager local field factors default back to those of the Lorenz–Lorentz model. The z component of the index of refraction is given by (recall that both chromophore and host polymer contribute) eqn. (6)

$$(n_z)^2 = 1 + 4\pi[\chi^{(1)}(c) + \chi^{(1)}(\text{polymer})] =$$
$$(n_{z0})^2 + 4\pi f_z(\omega)N\alpha[L_2(\mu f_p E_p / kT) - 1/3] \quad (6)$$

where $n_{z0} = \{1 + 4\pi[\chi^{(1)}(\text{polymer}) + \frac{1}{3}Nf_z(\omega)\alpha]\}^{1/2}$ is the linear index of refraction in the absence of the electrical poling field. For some device configurations, such as the birefringent modu-

lator, r_{13} as well as r_{33} defines device response. The expression for this component is somewhat more complicated than that for r_{33} but the analysis of other components of r and n follows the general prescription outlined above.

The above results predict that the electro-optic coefficient will increase in a linear manner with chromophore number density (loading) in the host polymer matrix. The slope (rate of change of electro-optic coefficient with number density) is defined by the product $\mu\beta$. Number density can be expressed in terms of chromophore/polymer weight fraction and chromophore molecular weight (M). Thus, commonly used chromophore figures of merit include $\mu\beta$ and $\mu\beta/(M)$, see Fig. 2. As seen in Fig. 4, plots of electro-optic coefficient *versus* chromophore number density for chromophores characterized by large dipole moments and polarizabilities frequently exhibit maxima.[23] Moreover, the maxima shift to lower chromophore loading values as the dipole moment and the polarizability of the chromophore increase.[23] The exact behavior of plots of electro-optic coefficient *versus* chromophore number density also depend on the shape of the chromophore. Such behavior is strongly suggestive of intermolecular electrostatic interactions playing a role in defining maximum realizable electro-optic activity. Table 2 provides the dipole moment, polariz-
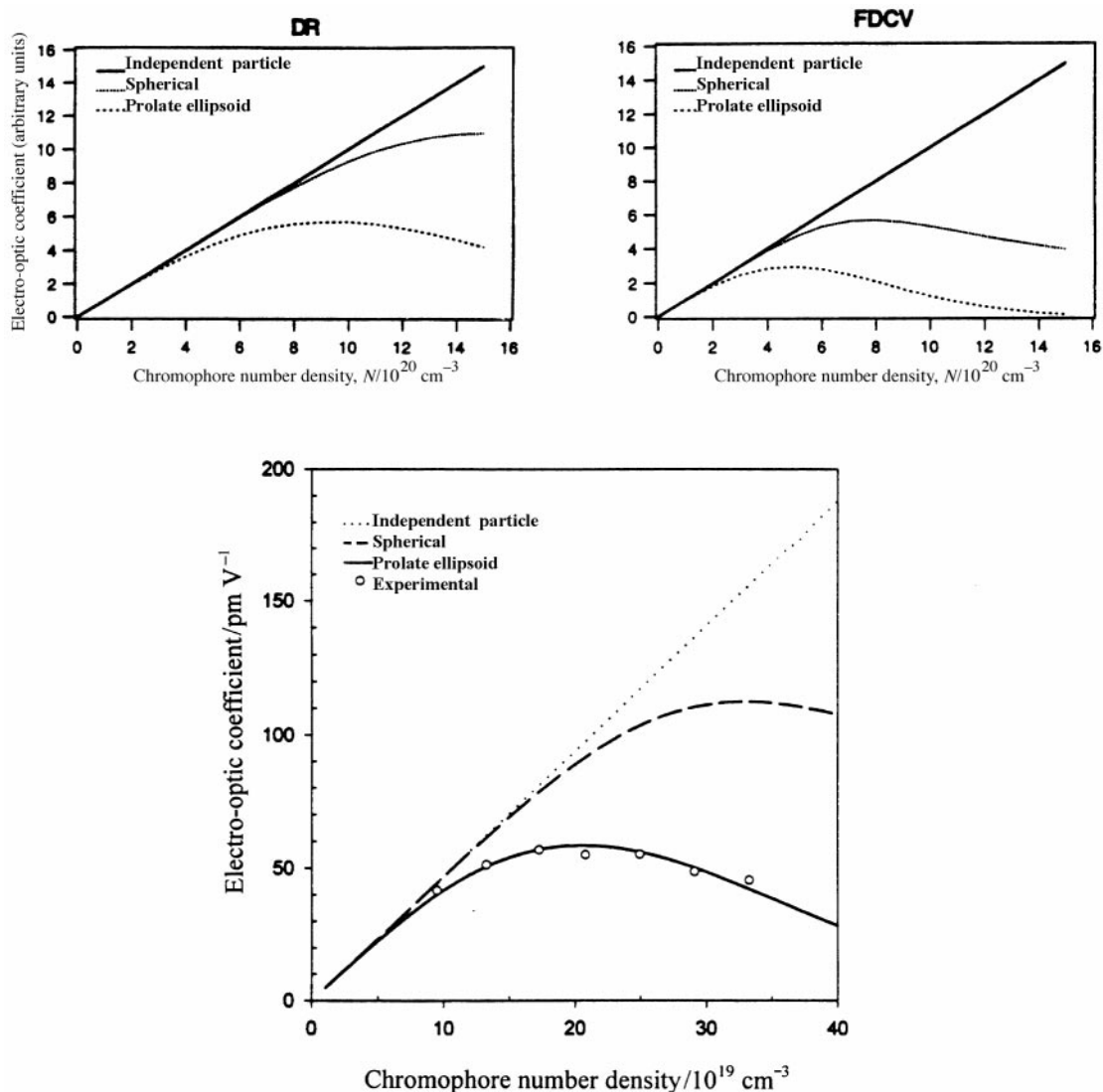
Fig. 4 The theoretically predicted variation of electro-optic coefficient with chromophore number density for three samples: DR, FDCV, and FTC. Models used in these calculations include neglect of intermolecular electrostatic interaction (linear dependence), treatment of electrostatic interactions but a hard sphere approximation applied to chromophore shape, and treatment of electrostatic interactions with approximation of chromophore shape as a prolate ellipsoid. The electro-optic coefficient axes for the DR and FDCV chromophores are arbitrary. Experimental data are also shown for the FTC chromophore. For detailed comparison of experimental and theoretical data for a number of chromophores the reader is directed to ref. 23.

Table 2 Magnitudes of electrostatic interactions for various chromophores[a]
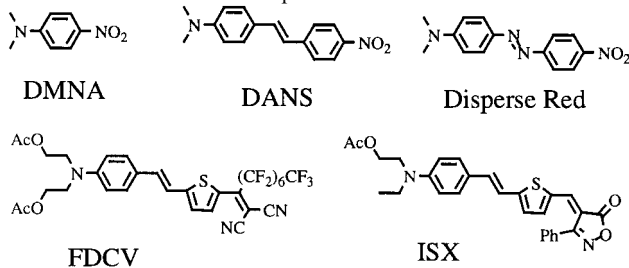
Chromophore	μ/D	$\alpha/10^{-23}$ cm^3	$I/10^{-19}$ J	$\beta/10^{-30}$ esu	U_{dd}/kJ mol^{-1}	U_{di}/kJ mol^{-1}	U_{ii}/kJ mol^{-1}	U_{total}/kJ mol^{-1}
DMNA	6.4	2.2	9.04	9.7	−2.46	−0.204	−0.372	−3.03
DANS	6.6	3.4	8.70	55	−2.78	−0.336	−0.855	−3.97
DR	7.0	3.8	8.26	55	−3.52	−0.422	−1.01	−4.96
ISX	8.0	7.6	7.90	153	−6.01	−1.10	−3.88	−10.99
FDCV	9.0	10.3	7.77	201	−9.62	−1.89	−7.01	−18.52

[a]Energies were calculated for per mol of dimers and for a 9 Å chromophore separation distance. For comparison, the thermal energy at 100 °C is 4.65 kJ mol^{-1}.

ability, ionization potential, and first hyperpolarizability for representative chromophores. Also, shown are values of dipole–dipole, induced dipole, and dispersion intermolecular electrostatic interactions between two chromophores calculated following London.[24] Clearly, as one proceeds down this table it becomes clear that intermolecular electrostatic interactions begin significantly to exceed thermal energies and are thus likely to influence poling-induced order. The simple existence of dipole–dipole interactions suggests that intermolecular electrostatic interactions will be spatially anisotropic and hence chromophore shape may be important.

Owing to the large magnitude of intermolecular electrostatic interactions their theoretical treatment is not simple. It can quickly be realized that simple pairwise treatment of interacting chromophores is not adequate to explain the experimentally observed results. The problem is thus a many body problem and quantum mechanics *per se* is not adequate for gaining quantitative insight into the experimental order parameter $<\cos^3\theta>$. One can propose a thermodynamic treatment, as suggested by Katz *et al*,[25] but such a treatment has the disadvantage of providing little insight into the relationship of molecular structure to the attenuation of optical non-linearity. Statistical mechanics seems the logical approach; however, a large number of rotational matrices are required to relate the chromophores to each other and to the electric poling field (laboratory axis). The simple integral of eqn. (5) becomes complex, requiring evaluation over many orientational variables. Approximate treatment of integrals over at least some of the orientational variables is called for particularly if an analytical solution is to be obtained. Consider the coordinate systems shown in Fig. 5 which relate a reference chromophore (denoted '1') to an applied electric field and to all other chromophores. It is necessary to compute the effective field felt by this reference chromophore from all other chromophores. We position all other chromophores in a simple lattice (see Fig. 5), where the inter-chromophore distance is fixed by the chromophore number density (*i.e.* N is proportional to r^{-3}), and place our reference chromophore at the center. A 'director' axis is defined by a vector connecting the reference chromophore to other chromophores positioned along a given director direction. We then follow Piekara[23] and average over the orientational variables associated with the other chromophores ('2' to '*n*'). This is analogous to the orientational averaging carried out by London.[24] The end result is that we are left with an intermolecular electrostatic interaction energy, U_2, depending on a single angle, θ_1, namely, $U_2 = -W\cos(\theta_1)$. Now the potential function to be used in our computation of $<\cos^3\theta>$ becomes $U = U_1 + U_2 = -\mu f_p E_p \cos\theta - W\cos(\theta_1)$.
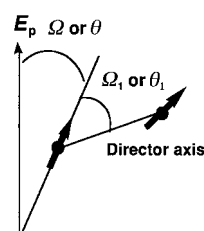

Fig. 5 The axes systems relating chromophores to each other and to the applied electric poling field. The rotation matrix Ω or angle θ relates reference chromophore 1 to the laboratory axis (electric poling field direction). The director axis between chromophore 1 and other chromophores contributing to the field felt by 1 is related to the principal axis of chromophore 1 by the rotation matrix Ω_1 or the angle θ_1. The director axis is related to the laboratory axis by the rotation matrix Ω'.

The evaluation of orientational integrals is facilitated by use of the trigonometric identity $\cos\theta = \cos\theta'\cos\theta_1 + \sin\theta'\sin\theta_1 \cos(\phi_1 - \phi')$. Although we must evaluate a number of integrals, an analytical expression can be obtained in the limit of treating chromophores as hard spheres, namely eqn. (7)

$$<\cos^3\theta> = (\mu f_p E_p/5kT)[1 - L^2(W/kT)] \qquad (7)$$

where L is the Langevin function (now expressed in terms of W/kT) and W is approximately the intermolecular electrostatic interaction energy defined by London.[24] Explicitly, W includes contributions from dipole–dipole, induced dipole, and dispersion interactions; it depends on r^{-6} where r is the average separation of chromophores in the point dipole approximation.[24] At first consideration, it might seem that a double thermal averaging has been carried out but in point of fact this aspect of our approximate treatment can be justified by more rigorous treatment. The London W exhibits a quadratic dependence on chromophore number density (loading in the polymer matrix). The term in brackets has the form of an attenuation factor that will decrease the acentric order parameter with increasing chromophore concentration. The above expression provides a qualitative explanation of the appearance of a maximum in plots of electro-optic coefficient *versus* chromophore number density. From consideration of Fig. 4, it is clear that the above expression and more sophisticated calculations carried out considering non-spherical chromophore shapes also qualitatively reproduce trends observed for variation of intermolecular electrostatic interaction energy and chromophore shape.

Theory predicts that a logical approach to improve maximum achievable electro-optic activity is to derivatize

naturally prolate ellipsoidal chromophores with bulky inert substituents to make chromophores more spherical. We have carried out simple preliminary modifications of several chromophores employing alkyl and aryl substituents.[23] In all cases, we have observed an increase in maximum achievable electro-optic activity.[23] A more systematic approach, that has not yet been demonstrated, would be to follow a dendritic approach to chromophore modification (see Fig. 6).

The agreement between theory and experiment is a necessary but not sufficient condition for a useful theory. It should be noted that the simple treatment discussed here is not likely to be useful for understanding behavior at high chromophore loading where significant 'non-transient' chromophore aggregation occurs. Such aggregation can lead to significant light scattering and optical loss (>5 dB cm^{-1})[26] and requires molecular dynamical considerations to be added to our theoretical treatment. For low to modest chromophore loading (the concentration range of focus in our above theoretical discussion) aggregation is not a problem and equilibrium statistical mechanical calculations provide an adequate description of observed phenomena.

Derivatization of chromophores with inert (sigma electron only) substituents to improve electro-optic activity also leads to delayed onset of light scattering due to chromophore aggregation. There may be two components to this observed phenomena; namely, (1) inhibition of chromophore close approach that limits intermolecular electrostatic interaction and hence aggregation and (2) improved chromophore/polymer interactions (better compatibility due to improved entropy of mixing and improved chromophore/polymer intermolecular electrostatic interactions).

An understanding of the role of chromophore–chromophore intermolecular electrostatic interactions in limiting achievable electro-optic activity has led to the realization of polymeric electro-optic coefficients that exceed those of lithium niobate. Values for r_{33} in the range 55 to 84 pm V^{-1} have been realized for the FTC[27] and CZC[28] chromophores of Fig. 2. Such values of electro-optic coefficient have permitted V_π values of the order of one volt to be obtained for Mach Zehnder and birefringent modulators. Systematic modification of existing chromophores such as FTC and CZC should permit electro-optic coefficients of the order of 100 pm V^{-1} to be obtained which should in turn permit realization of V_π voltages of less than 1 V.
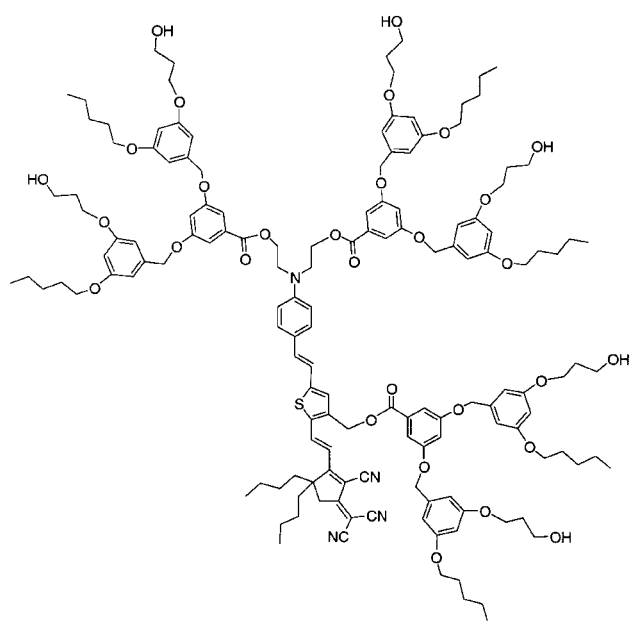

Fig. 6 A dendritic approach for inhibiting unwanted close approach of interacting chromophores.

The drive voltage, V_π, depends upon electrode spacing and the conductivity of cladding layers, also on device length, L. Researchers at Lockheed-Martin have made significant progress in producing cladding layers of desired conductivity.[29] Advances in this area and in the development of novel device architectures should further reduce drive voltage requirements.

A number of more subtle factors can influence the magnitude of electro-optic activity that can be realized by electric field poling. Obviously, the strength of the electric poling field that can be employed is limited by material dielectric breakdown. Ionic impurities can lead to conductivity that also limits the maximum achievable field felt by the chromophores.[30] Removal of impurities by repeated recrystallization of chromophores and purification of polymers usually eliminate problems associated with ionic conductivity. Some materials, containing highly polarizable chromophores and polymer matrices (such as poly(*p*-phenylenes)) where electronic charge transport is facilitated, exhibit significant photoconductivity. This photoconductivity forces poling to be carried out in the dark.[30]

Stabilizing macroscopic electro-optic activity: lattice hardening

As noted above, electro-optic activity induced by electric field poling must be stable at temperatures encountered in device fabrication and operation. This implies long term stability for operating temperatures as high as 125 °C and short term stability for temperatures approaching 200 °C. Two strategies for achieving high thermal stability of poling-induced electro-optic activity have been pursued.[20] The first is to prepare chromophore/polymer composite materials where the polymer is a high glass transition temperature (T_g) polymer such as a polyimide. Acentric chromophore order is induced by poling the chromophore/polymer composite material near its glass transition temperature. Cooling the material to room temperature, in the presence of the electric poling field, locks in the poling-induced electro-optic activity. A number of workers have shown that the thermal stability of electro-optic activity for such materials can be correlated with the difference between the operating temperature and the glass transition temperature of the composite material.[20] There are several disadvantages of such chromophore/polymer composite materials including: (1) poor solvent compatibility for chromophore and polymer and for chromophore with the host polymer leading to low values of maximum achievable loading, (2) chromophore phase separation and aggregation with processing (*e.g.* spin casting) and aging, (3) sublimation of chromophores during electric field poling at high temperatures, (4) chromophore migration and phase separation during electric field poling, (5) loss of chromophores with application of cladding layers due to chromophores dissolving in the spin casting solvent, (6) poor solubility of high T_g polymers such as polyimides in traditional spin casting solvents leading to poor optical quality films due to difficulty of viscosity control, (7) plasticization of the host polymer with increased chromophore loading, (8) increased demands on chromophore chemical stability with high temperature poling and non-traditional solvents, and (9) rapid relaxation of chromophore poling-induced order due to poor coupling of the chromophore to the polymer dynamics (*e.g.* chromophores existing in void regions). Many of the aforementioned problems can be alleviated by covalent attachment (including single point attachment) of the chromophore to the polymer backbone.

The second approach is to make use of covalent coupling of chromophore and polymer and to effect some sort of lattice hardening (either intramolecular chain stiffening or intermolecular crosslinking) during the later stages of poling.[31] The chromophore may either be attached (tethered) to the polymer backbone[32] or incorporated into the backbone.[33] The chromo-

phore may also be functionalized to mimic one of the monomers in a traditional lattice hardening processing such as the formation of sol–gel glasses.[34] Indeed, one of the most widely used approaches is to prepare chromophores terminated by reactive hydroxy groups that can be used to produce three dimensional crosslinked polyurethanes through oligomer growth and coupling chemistry.[35] This latter approach has the advantage of permitting high chromophore loading; however, care must be exercised in maintaining reactant stoichiometry at 1 to 1 for hydroxylated chromophores and isocyanate containing coupling reagents to avoid phase separation (and resultant optical loss due to light scattering).[36] Since poling and lattice hardening are both temperature-dependent processes, optimum electro-optic activity and lattice hardness are usually achieved using a protocol wherein temperature and electric field are increased in a series of steps.[34,35] An initial temperature jump increases chromophore mobility and permits the chromophores to reorient in the presence of the applied electric field. The increase in temperature drives further crosslinking which ultimately stops chromophore reorientation in the field requiring another temperature increase. Application of too great an electric field to a soft lattice causes material damage and increases optical loss. Thus, a stepped protocol also greatly reduces poling-induced optical loss.[36]

The major disadvantage of sol–gel and polyurethane (PU) oligomerization reactions for achieving hardened acentric chromophore lattices is the requirement for careful control of reaction conditions. For example, atmospheric moisture can lead to non-stoichiometric reaction conditions, phase separation, and optical loss.[36] Such control is not always easily transitioned to preparation of bulk materials for device manufacture.

The double-end crosslinkable (DEC) chromophore scheme,[32] where a processable precursor polymer is prepared in a first step and the second end of the chromophore is coupled to the polymer lattice during poling, provides some de-coupling of spin casting and poling steps from the process of lattice hardening. If photo-induced crosslinking could be utilized to secure the second end of the chromophore, the lattice hardening process would be completely de-coupled from the temperature-dependent poling process.[20] However, to the present time, absorption by the non-linear optical chromophore has interfered with absorption by the photo-initiator to an extent to make such hardening ineffective.[20]

Two methods have been developed to evaluate the thermal stability of poling-induced electro-optic activity. The first simply involves monitoring electro-optic activity as a function of time. An example of this type of assessment is provided in Fig. 7. An obvious disadvantage of such type of assessment is the time required for measurement even when elevated temperatures are employed to hasten relaxation. A more rapid analysis involves ramping the temperature while monitoring second order optical non-linearity (second harmonic generation is conveniently used for this purpose[18]). Such an experiment is the non-linear optical analog of thermal gravimetric analysis (TGA) except that loss of acentric order and not material decomposition is monitored. In Fig. 8 we show the results of such dynamic analysis of thermal stability of electro-optic activity for a variety of electro-optic materials. It is clear that attachment of the chromophore to the polymer backbone produces a dramatic improvement in the stability of poling-induced electro-optic activity. Attachment of both ends of the chromophore to the polymer lattice results in further improvement in thermal stability. Excellent thermal stability can be achieved with a variety of approaches. Sol–gel hardening schemes typically yield materials that show a gradual loss of electro-optic activity with increasing temperature. This is to be expected as sol–gel reactions cannot be driven to completion for temperatures achievable with the stepped poling protocol discussed above. The partially densified sol–gel materials, together with the temperature-dependent sol–gel chemistry, lead to the data shown in Fig. 8. Multi-phasic behavior can be observed reflecting the heterogeneity of crosslink density in the material.

Controlling optical loss in electro-optic materials

Optical loss in polymeric electro-optic waveguides has been measured either by the cut-off method or by a liquid out-coupling technique.[37] Optical loss can be classified either as loss due to absorption of light or due to scattering of light from index of refraction inhomogeneities with dimensions of the order of the wavelength of light. Absorption loss can arise either from the absorption tail of the interband (HOMO−LUMO) absorption or from absorption associated with vibrations of the C–H group. The latter can be attenuated by partial replacement of hydrogens with fluorines. As a minimum in the vibrational absorption is observed near 1.3 μm, operation at this wavelength poses little problem for loss from vibrational absorption (i.e. absorption losses are typically less than $1\,dB\,cm^{-1}$). For operation at 1.55 μm, C–H vibration absorption from both chromophore and polymer typically leads to losses above $1\,dB\,cm^{-1}$ and partial fluorination is required to reduced losses to $1\,dB\,cm^{-1}$ or less. Significant optical loss from interband absorption can be avoided by maintaining a large wavelength offset between the
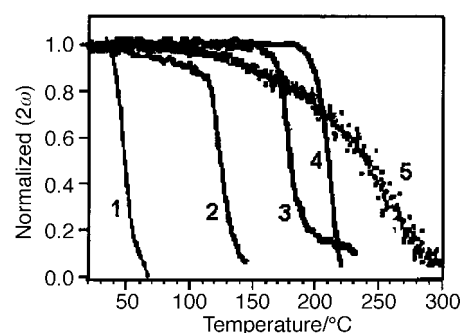
Fig. 8 The dynamic thermal stability of second order optical non-linearity for a number of materials: 1, a polymer containing the DR19 chromophore (see Fig. 2) as a pendant; 2, a PU-DR19 thermosetting material with only one end of the chromophore attached to the polyurethane lattice;[35] 3, a DEC type DR (LD-3) chromophore coupled at both ends to a poly(methyl methacrylate) (PMMA) type lattice;[32] 4, a DR chromophore with both ends coupled to a heteroaromatic (polyimide-like) polymer lattice;[31] 5, a DR chromophore with both ends coupled to a sol–gel glass lattice.[34] Second harmonic generation is used to assess second order non-linear optical activity. The heating rate is approximately $5\,^{\circ}C\,min^{-1}$.
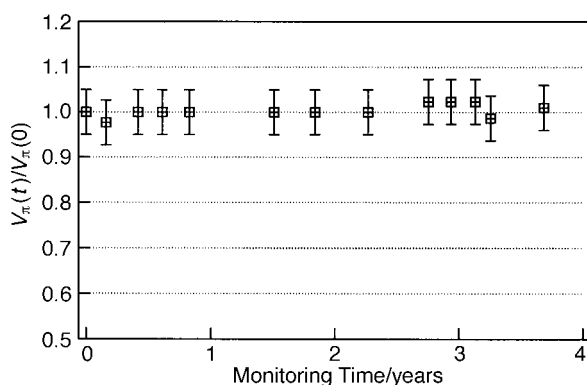
Fig. 7 The thermal stability of the drive voltage for a Mach Zehnder modulator fabricated from PU-DR19 is shown. The test was started by TACAN Corporation on 21st July, 1995. No change in V_{π} has been observed to the present time.

operating wavelength and the wavelength of the interband absorption maximum. Thus, loss due to absorption can usually be avoided by appropriate chromophore and polymer host design.

Optical loss due to scattering represents a much more complex problem that requires a much more determined effort to achieve electro-optic device structures characterized by optical loss of 1 dB cm^{-1} or less. As already noted, optical loss due to scattering can be associated with heterogeneity of index of refraction in materials. Scattering increases dramatically as domain sizes approach the wavelength of light being used in various applications. Index of refraction heterogeneity can arise from fundamental material component (chromophore/polymer) incompatibility or from processing-induced loss. Processing-induced losses can be associated with spin casting, electric field poling, waveguide fabrication, and/or cladding layer deposition of thin films. As will be discussed later, optical loss can also be associated with transitioning light into and out of polymeric electro-optic modulator waveguides (i.e. the problem of impedance matching of silica fiber and polymeric waveguides).

As already noted, chromophore composite materials are particularly prone to phase separation leading to high optical loss and poor loading densities. The utilization of chromophore/polymer composites appears to have been abandoned by all but a few companies restricted to use (by blending) of off-the-shelf chromophores and polymers. Accordingly, our remaining comments will be restricted to materials where chromophores are covalently attached to polymers or where materials are prepared by covalent coupling of monomers (and oligomers) to form three dimensional crosslinked chromophore/polymer lattices.

The first processing step that can affect optical quality is that of spin casting of the unpoled polymer film. The issue here is solvent choice, as the solvent must lead to appropriate viscosity, be compatible with chromophore and polymers, and be capable of being completely removed from the final film. For thermosetting monomer/oligomer materials and for low T_g hydrocarbon polymers, finding a spin casting solvent that yields high quality optical materials is rather straightforward. However, the process is not so readily accomplished for high T_g polymers such as polyimides or for polymers with high fluorine content (prepared to suppress C–H vibrational absorption at 1.55 μm). Of course, spin casting must be carried out in a dust free environment as dust particles can lead to significant light scattering and optical loss. Various modifications of clean room procedures normally alleviate this loss contribution.

Optical losses associated with electric field poling can be even more diverse. A major, but avoidable, component of poling-induced loss is associated with surface damage of polymer films arising from applying too high a voltage (particularly with corona poling) to a polymer film that is too soft.[36] This component of poling-induced loss can be reduced to insignificant values by employing stepped poling protocols where field strength is increased in a stepwise manner as the polymer lattice is hardened.[36]

Another component of poling-induced loss that is also easily avoided is that of chromophore migration and phase separation occurring during the poling of composite materials. Covalent attachment of the chromophore to the polymer normally eliminates this type of loss.

Since electric field poling acts to modify the index of refraction (e.g. causing the n_z and n_y indices to diverge) by influencing the chromophore orientational distribution, inhomogeneity in the local poling field can lead to light scattering. Such local field variations might arise from the presence of air bubbles associated with solvent evaporation. Teng and co-workers[37] have developed a quantitative theory for accounting for this component of poling induced optical

loss. The variation of the index of refraction associated with transverse magnetic (TM) optical mode polarization, δn_z, can be shown to be proportional to $5\pi\alpha(n_z)^8(\delta f_p)^2(r_{33})^2/\{9\beta^2 n_0 N[f_z(\omega)]^3[f_z(0)]^2\}$. The principal electro-optic coefficient is defined by eqn. (3). The total optical power scattered can be shown to be proportional to $(\delta n)^2 n^2(\delta V)^2\lambda^{-4}$ where δV is the volume element that experiences a different local poling field $\delta f_p E_p$. Thus, the waveguiding loss per unit length of polymeric electro-optic waveguide for the TM optical mode is predicted to increase as $(r_{33})^4\lambda^{-4}$. The TM waveguiding loss is approximately four times greater than the transverse electric (TE) mode (δn_y associated) waveguiding loss. Teng and co-workers[37] have demonstrated reasonable agreement between experiment and theory for the samples that they investigated. At first this might seem distressing as it could be incorrectly interpreted as an unavoidable relationship between electro-optic activity and poling-induced optical loss. In point of fact, the loss mechanism discussed by Teng and co-workers[37] is based on the presence of material defects. As those defects are reduced (e.g. by improved control of spin casting conditions) optical loss goes down. Moreover, it is clear from a consideration of the theory of Teng and co-workers[37] that their optical loss mechanism is independent of the hyperpolarizability of the chromophores although a more isotropic polarizability will decrease optical loss from their mechanism. Thus, their loss mechanism does not penalize the use of high β chromophores.

Our experience is that poling-induced optical losses can be reduced to insignificant values (e.g. ≪1 dB cm^{-1}) by careful control of spin casting and poling conditions.[36] Maintenance of material homogeneity is critical, including by avoiding dust particles and voids and by avoiding phase separation during spin casting, poling, and lattice hardening.

Post poling optical losses are most commonly associated with surface pitting during reactive ion etching (RIE) of channel or ridge waveguides and during the deposition of cladding layers.[38] Losses from both of these processes are attenuated by realization of adequate lattice hardness (high polymer crosslink density). Of course, choice of conditions (type and kinetic energy of reactive ions in RIE and spin casting solvent in cladding layer deposition) influences optical loss. For example, Steier and co-workers[38] have shown that reducing the kinetic energy of reactive ions can reduce associated optical loss (from waveguide wall roughness) to the order of 0.01 dB cm^{-1}.

Vertical integration of polymeric electro-optic waveguide circuitry with VLSI semiconductor electronic circuitry poses the problem of avoiding optical loss associated with the underlying irregular topology of VLSI wafers.[6] Fortunately, such optical loss can be essentially eliminated by using planarizing polymers. Vertical integration has the advantage of permitting very high densities of modulators to be achieved. Vertical transitions have the advantage of minimizing optical loss associated with electro-optically active waveguide sections.[6,39] Light can be routed between passive and active waveguides using vertical transitions. Light propagation in a high loss active waveguide is thus minimized. This aspect of loss management is illustrated in Fig. 9.

In summary, material optical loss is probably the most demanding aspect of the fabrication of polymeric electro-optic waveguide devices. The good news is that with careful design of component materials and careful control of processing conditions optical loss values in the range 0.7 to 1.2 dB cm^{-1} can be consistently achieved. Such values are adequate for most device applications. Loss values of this magnitude, while superior to that achieved with GaAs, are not as low as those achievable with lithium niobate. For very low loss values to be achieved even more dramatic modification of materials (replacement of more hydrogens with fluorines) and control of processing conditions must be effected for polymers.
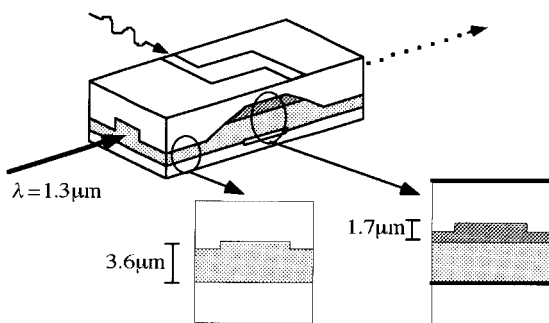
$\lambda = 1.3 \mu m$

$3.6 \mu m$ $1.7 \mu m$

Fig. 9 The schematic and scaled cross-sections of waveguide segments of a low-loss hybrid polymeric electro-optic modulator.

Fabrication of buried channel waveguides: from simple waveguides to vertical transitions

Two general approaches have been employed to fabricate buried channel polymeric electro-optic waveguides (a channel of material of high refractive index surrounded by materials of lower index of refraction): (1) reactive ion etching and (2) multi-color photolithography.[6,20,38] The latter has the advantage of requiring fewer steps and permitting buried channel waveguide structures to be fabricated without deposition of an upper cladding layer. The disadvantage of multi-color photolithography is the requirement for a photoactive species that gives the desired photo-induced change in index of refraction. As various aspects of these two fabrication techniques have been treated in other publications[20] they will not be reviewed here. Rather we focus on more recent and more sophisticated aspects of waveguide fabrication associated with complicated waveguide structures required in vertically integrated device structures.

One of the advantages of optical polymer technology is the ability to utilize different types of polymers within the same integrated optical circuit to perform specific functions.[6,39] For example, electro-optic or light amplifying polymers (including light harvesting/amplifying polymers) can be integrated with low loss passive polymers to provide low optical loss interconnections. Passive polymers, specifically designed for very low optical loss, have been used to fabricate waveguides exhibiting optical losses as low as 0.1 dB cm^{-1} at 1.3 μm wavelength.[40] Owing to the reasons already noted, active (chromophore-containing) polymer waveguides typically exhibit greater loss than passive polymers. Thus, an ideal circuit involves light spending no more time in active waveguide segments than necessary for signal processing. While adhesion and patterning issues can be important for wedding different polymers, the greatest difficulty in the integration of active and passive polymers relates to achieving mode matching.[41] The optimum optical mode pattern in passive waveguides is usually nearly circular while that in an electro-optic modulator waveguide is a relatively flat ellipse.[42] This mismatch in mode shapes and difference in index of refraction of the active and passive polymers means that the two waveguides cannot be simply butted together. The use of the third vertical dimension provides a method of integrating passive and active polymers that solves the mode matching problem. In the approach that we have employed the interconnect waveguide is first fabricated in a low loss passive polymer system. The active polymer is then placed on top of this layer and patterned into the area where needed. Vertical coupling structures are then fabricated to channel the light up into the active polymer and then back down again into the passive waveguide. Such a design is shown in Fig. 9. The passive waveguide was designed to provide close mode match to the standard 9 μm core silica transmission fiber for fiber coupling (see next section). The critical fabrication technology is the etching of the vertical taper that was designed adiabatically to couple light to the higher index upper (electro-optically active) core layer. Vertical tapers can be reactive ion etched using O_2 and CF_4 either directly by shadow masks or through intermediate patterned photoresist layers. These techniques create vertical slopes whose height can be accurately controlled from 1 to 15 μm and whose length can be set from 100 to 2000 μm.[43] A voltage applied to the electrodes will phase modulate light or, if configured as a Mach Zehnder interferometer, will amplitude modulate light. In the modulator section, the passive core layer serves as the lower cladding to the active waveguide. After modulation, the power again transfers to the passive core for further routing. Both the adiabatic slopes and the lower electrode serve as inherent mode filters to minimize stray light that exists in the device. While the mode in the passive waveguide was designed to be symmetric for good fiber coupling, the mode in the modulator was designed to be tightly confined to the active layer for good modulator efficiency (low V_π operation). Evaluation of such modulators indicates that no sacrifice in electro-optic efficiency occurs. Also, highly efficient coupling of light into and out of the active layer occurs.[44]

While we do not review in depth the photochemical processing of waveguides, some comments concerning maskless fabrication of channel waveguides by simultaneous direct laser writing and electric field poling are appropriate. This approach is an outgrowth of laser-assisted poling.[45] Electro-optic materials based on photochromic molecules, such as 4-amino-4'-nitroazobenzenes, are unique in that short wavelength visible or ultraviolet radiation can alter the alignment of chromophores in the material to change both the index of refraction and the degree of alignment during poling. Based on these effects, one can simultaneously directly laser-write and (electric field) pole a pattern of arbitrary channel waveguides that are electro-optically active only in selected regions.[46] The sample to be written with channel waveguides consisted, in our initial work, of a substrate, gold ground electrode, three spun layers of polymer (upper and lower passive cladding layers and active core), and a semi-transparent upper electrode. For fiber coupling, the endfaces of the sample are either cleaved or cut with a dicing saw before waveguide writing. The core layer was fabricated from a disperse red 19 (DR19) chromophore-containing, polyurethane-thermoset polymer.[35] The absorption maximum of the DR19 chromophore is at 470 nm. Waveguide writing is carried out with a focused beam of 488 or 515 nm light from a continuous wave argon ion laser. When a beam of visible light is scanned across the sample in the absence of an applied poling field (or in an area outside the top electrode) the chromophores in the path of the beam are preferentially aligned perpendicular to the substrate with, on average, equal numbers of chromophore dipoles pointing up and down.[47] Chromophore reorientation is driven by photo-induced *trans-cis-trans* isomerization. Centrosymmetric chromophore order is induced consistent with the applied optical field direction and the symmetry of the chromophore optical transition moment. The partial centric chromophore order increases the refractive index for TM optical mode polarization and a passive channel waveguide that only supports the TM mode is obtained. When the laser beam scans across the area covered by the semi-transparent top electrode and with the electric (dc) poling field on, the chromophores are preferentially aligned (acentrically ordered) in the direction of the electric poling field. This latter process is referred to as laser-assisted poling and results in an electro-optic channel waveguide. The waveguides are written using a binocular microscope with the writing beam fed through one eyepiece and focused on the sample. For the example that we consider here, the spot size of the beam on the sample is adjusted from 1 to 50 μm and the typical unpolarized writing beam power was 1 mW. An electric poling field of 100 V μm^{-1} was used. During the writing the substrate temperature was elevated further to

promote chromophore reorientation. Note that isomerization and molecular rotation are both inhibited by intermolecular interactions so increasing the temperature increases both processes. The *trans-cis-trans* isomerization can be viewed as a low activation energy pathway to molecular reorientation (*i.e.* rotation). For the 4-amino-4′-nitroazobenzene (DR19) chromophore of the present example this laser-assisted poling process leads to an electro-optic coefficient (at 1.3 μm operating wavelength) of 17 pm V^{-1} (corresponding to a V_π value of 8 V in a 25 mm long device). This laser-assisted poling value is considerably higher than the value of 5 pm V^{-1} obtained under the same conditions (100 V μm^{-1} poling field) without laser assistance. The technique is thus a fast and effective method to prototype new electro-optic devices. It requires no lithography mask and can produce higher electro-optic coefficients than with conventional electrode poling. Laser-assisted poling can be further refined by using variable laser wavelengths (multi-color laser-assisted poling). Of course, the severe limitation of this technique is the reliance on the use of chromophores that can undergo photo-induced *trans-cis-trans* isomerization.

Mode matching of polymeric EO waveguides to silica fibers

The design criteria for active and passive waveguides are different. Passive waveguides, which typically are spherical graded index waveguides with core diameters of 8–10 μm, are designed for minimum optical loss. Active (electro-optic) waveguides, on the other hand, are designed to minimize drive voltage requirements. Thus, active waveguides typically have a width of approximately 5 μm and a height of 1–2 μm. A high index of refraction contrast between active and cladding layers is used to confine the optical mode in the active region. The mode in such a waveguide is elliptical. Butt coupling active and passive modes will lead to optical losses of greater than 4 dB per transition.

The obvious solution to this optical loss problem is to create a tapered transition that allows the optical mode to expand as it transitions from the active to passive waveguide regions.[42] Such transition tapers (mode transformers) are readily fabricated by reactive ion etching techniques using gray level lithography, shadow ion etching, or offset lithography.[42] With these techniques and oxygen reactive ion etching, one can fabricate vertical slopes characterized by a range of parameters: lengths ranging from 50 to 2000 μm, heights ranging from 1 to 15 μm, and slope angles ranging from 0.1 to 10°. We have reliably fabricated multiple waveguide bends that exhibit excess loss of 0.2 dB or less. Mode transformers reduce coupling losses by several decibels, leading to losses approaching 1 dB per transition. Such reduction of optical loss associated with silica fiber to polymeric electro-optic waveguide coupling is necessary if polymeric electro-optic modulators are to compete with lithium niobate modulators where insertion losses are on the order of 4 dB total insertion loss. It should also be noted that the coupling loss problem can also be simplified by utilizing silica fiber (HE980 5 μm) of reduced core diameter compared to normal diameter silica fiber (SMF-28 and PM 9 μm). Recently, TACAN Corporation[48] has proposed an alternative mode transformer to the one introduced by us. Their transformer reduces losses per transition (facet) by approximately 3 dB.

Vertical and horizontal integration of modulators with VLSI semiconductor electronics

The fabrication of polymer integrated optics devices relies on spin casting which is amenable to large area coverage of inexpensive substrates such as silicon. This means that large area, complex integrated optical circuits and devices can be built with relatively low cost. However, several technical problems must be faced particularly for vertical integration. One of the most serious of these is the irregular topology of VLSI circuitry. Deposition (spin casting) of an electro-optic polymer layer immediately on top of this circuitry would lead to unacceptable optical loss for the electro-optic circuitry. Fortunately, this problem can be addressed by spin casting about 6 μm of planarizing polymer (PC3–6000 from Futurrex) on top of the VLSI circuitry.[42] At temperatures near 200 °C, PC3–6000 reflows from peaks to the troughs and further smooths the rough (1–6 μm) VLSI features to variations of less than 0.2 μm. Electro-optic circuits fabricated on top of the planarized layers exhibit optical loss values indistinguishable from those fabricated on polished silicon (somewhat less than 1 dB cm^{-1}).[42]

A second challenge that must be faced is the protection of VLSI circuitry during electric field poling of the electro-optic polymer. We have shown that with adequate grounding such poling can be accomplished without detectable effect on the performance (*I–V* curves) of underlying semiconductor VLSI circuitry.[42]

A third issue that must be addressed is that of making connections between VLSI electronic and polymeric electro-optic circuitry. This translates into the need to make deep and precisely controlled interconnection *vias* (channels) through the relatively thick planarizing polymer layer. We have accomplished this feat using a trilayer processing scheme and an oxygen RIE resistant material (spin on glass) to transfer the pattern (a normal photoresist is a poor mask for oxygen RIE).[42] A perfluoromethane plasma is used to etch the spin on glass.[42] This is followed by oxygen plasma etching of the deep vias in the planarizing polymer and deposition of metal electrodes connecting the VLSI and polymer EO circuitry.[42]

A number of multi-modulator packages ('opto-chip'), based upon integration of multiple birefringent or Mach Zehnder modulators, have been fabricated and evaluated.[42] Multiple modulator packaging has been achieved without degradation in the performance of either VLSI or electro-optic circuitry.[42] Crosstalk between adjacent modulators has to this point been undetectable, which implies isolation of greater than 50 dB.[42]

Fabrication and evaluation of prototype devices

Early prototype devices were typically single birefringent or Mach Zehnder modulators. Such devices have been operated to frequencies in the range 100–200 GHz and shown to have 3 dB bandwidths of approximately 350 GHz.[5] More recently, performance has been enhanced by improving the efficiency of transition of electrical signals from millimeter wave transmission structures to electro-optic modulator electrode (*e.g.* microstripline) structures.[49] Millimeter wave transmission lines from sources or from antennas are typically hollow rectangular metal waveguides whose cross sectional dimensions are of the order of a few millimeters. In contrast, the millimeter wave transmission line in a polymer modulator is a microstripline. To couple these two very different transmission lines requires novel broadband structures. We have recently designed and demonstrated an integrated anti-podal finline transition structure.[5] This structure has the advantage of low loss and high dimensional fabrication tolerance. The transition gradually transforms the electric field profile of the rectangular metallic waveguide to that of the microstripline and effectively couples power into the modulator. The finline structure must be inserted into the small W-band rectangular waveguide (1.25 by 2.5 mm) and therefore the substrate thickness must be kept as small as possible. We have chosen to use 127 μm thick Mylar film. This film was mounted on a silicon substrate for mechanical support during processing. A gold ground plane was deposited on the Mylar and employing standard photolith-

ography techniques the lower finline transition pattern was then etched in the region to be inserted into the waveguide. The lower cladding layer and the active polymer layer were spin coated on the substrate and the electro-optic polymer was corona poled. The optical waveguide pattern was defined in the polymer using reactive ion etching with alignment to the pre-etched ground pattern. The upper cladding was then spin coated on and a thin layer of chromium and gold was deposited to form the top electrode. A thick photoresist was patterned to define the top electrode and the upper finline transition region. Electrochemical gold plating was used to increase the thickness of the top electrode to 7 µm. The performance of an array of these modulators was evaluated to 100 GHz.[49] Fabrication of polymeric modulators on flexible substrates means that the modulator can be molded to a curvilinear surface such as that of a receiving antenna.

Another simple modulator is that of the push–pull Mach Zehnder modulator recently discussed by Wang *et al.*[50] Such a design configuration reduces the drive voltage requirement by a factor of two.

Mach Zehnder modulators with 3 dB directional couplers on their output instead of a Y junction act as very fast optical switches. The applied voltage toggles the output light between the two output waveguides. The balanced output modulator has applications both in digital and analog communications. If a sinusoidal modulation signal is applied and if the modulator is properly biased, the light from the two outputs are both sinusoidally modulated but are 180° out-of-phase. If both of these signals are transmitted over a fiber optic line and detected at the far end by a balanced detector the modulation signal can be extracted while the noise is cancelled.[51] Such applications of the balanced modulator require a very high extinction ratio between the two outputs. That is, when V_π is applied, light is 100% switched from one output to the other. To achieve this the output coupler must be very close to a true 3 dB coupler, *i.e.* the power from either input must be divided equally to the two output waveguides. The device is thus highly sensitive to fabrication errors in the waveguide width, etch depth, and refractive indices. We have found that fabrication defects can be corrected by *in situ* trimming.[52] Trimming of electro-optic devices structures involves photobleaching to alter the property of devices. Typically the bleaching beam is the 488 nm output of an argon ion laser. Using FT-IR spectroscopy, we have been able to confirm that photodecomposition has occurred in the trimming process.

In the case of trimming 3 dB couplers, the fabricated coupler is placed under a microscope and light is fiber-coupled into one of the inputs as the power from each of the two outputs is monitored. Bleaching light is delivered by a multimode fiber to one of the eyepiece bores of a binocular microscope. An eyepiece of the microscope was removed and the output end of the fiber was placed in the image plane of the objective lens. The microscope objective reduces the output pattern of the fiber and projects a beam spot onto the sample. The size of the fiber core, the magnifying power of the microscope objective lens, and the axial position of the fiber tip determine the spot size. Spot sizes from 1 µm to greater than 1 mm can be achieved. The position of the spot on the sample is observed through the other eyepiece or by a video camera on the microscope. Since the fiber tip is fixed to the microscope its image always appears at the same place in the observation field of view when moving the microscope.

To trim the directional coupler, the trimming beam spot is scanned for a fixed distance into the gap between the two coupling waveguides as the two outputs are monitored. The region scanned by the trimming beam has reduced refractive index, which reduces the distance the tails of the waveguide modes extend into this coupling region. This, in turn, reduces the coupling coefficient and changes the output state for the two waveguides. We have used trimming to optimize the

performance of ultrafast switches fabricated employing 3 dB couplers. These devices have been demonstrated by switching a 1 Gb s^{-1} digital data stream with complementary bit patterns on the two outputs.

We have also fabricated a variety of more complex electro-optic modulator based devices. Such fabrication will be illustrated here by the example of a wide band millimetre wave photonic phase shifter (see Fig. 10). Such photonic phase shifters will likely play a key role in large phased array radar antennas.[53] Phased array antennas are made up of a large number of radiating elements with the phase and amplitude of the radiation from each element under independent control. By varying the phase and amplitude, the pattern of the array can be electronically scanned or its radiation pattern modified to avoid unwanted signals. The ideal phase shifter should be voltage controlled, broadband, and lightweight. An attractive method of delivering these controlled signals to each antenna is the use of low loss optical fibers. The millimetre wave signal is modulated onto the optical carrier and transmitted by fiber to the antenna where an optical detector recovers the millimetre wave signal. Fibers are low loss, light weight and have the possibility of low noise optical amplification.

Our photonic phase shifter is composed of a Mach Zehnder interferometre within a Mach Zehnder interferometer. The millimetre wave signal is applied to each arm of the upper interferometer but with a 90° phase shift between the signals. If the amplitude of the drive signals is small the frequency of the output of this interferometer is the optical carrier frequency shifted by the millimetre wave frequency. A DC phase control voltage is applied to the other arm of the complex interferometer. The phase of the millimetre wave modulation on the optical carrier is thus controlled by the magnitude of the DC voltage. We have evaluated the performance of our photonic phase shifter using an optical carrier wavelength of 1.31 µm and a microwave frequency of 16 GHz. Nearly ideal performance behavior (phase shift linearly related to control voltage) was observed to voltages of the order of 8 V.[54]

The prototype devices that we have discussed thus far are fabricated from hardened electro-optic polymer materials and are operated at temperatures significantly below the glass transition temperature of the electro-optic polymer. No bias voltage is applied so that the only voltage applied to the electro-optic waveguide is a radiowave (microwave, millimetre wave) drive voltage. Since lattice hardening is never perfect, there is always some relaxation (loss) of electro-optic activity after the electric poling field is turned off. This could, for example, arise from chromophores existing in void regions where steric confinement from the polymer lattice is poor. An alternative to devices fabricated from such materials is a device where a constant device bias field of substantial magnitude (*e.g.* 50–200 V µm^{-1}) is maintained.[54] While this bias field maintains high acentric order, the modulating AC electric field
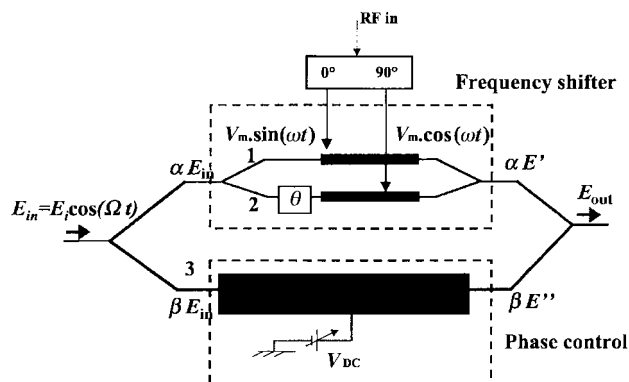

Fig. 10 The schematic diagram of a millimeter wave photonic phase shifter.

is applied. Such a device configuration makes use of the full electro-optic activity of the second order non-linear optical chromophore. For example, the FTC, APII, and DR chromophores (see Fig. 2) in poly(methyl methacylate) gave r_{33} values of 83, 70, and 22 pm V^{-1} respectively at a measurement wavelength of 1.31 µm. This simple constant bias device can be operated for long periods of time with no evidence of degradation in performance. It is difficult to say where this device configuration will find practical application; however, the configuration is useful for assessing the properties of polymeric electro-optic materials without concern (and correction) for relaxation of chromophore orientation.

Field test performance and comparison with the competition

TACAN Corporation has evaluated both birefringent and Mach Zehnder modulators (fabricated using disperse red chromophores) for CATV applications.[55] The performance characteristics of polymeric electro-optic materials have since improved significantly, particularly with respect to drive voltage requirement (using chromophores such as FTC and CZC) but also with respect to thermal and photochemical stability. However, the initial TACAN study provides a useful baseline against which to compare improvements in performance.

In their initial investigation, Shi et al.[55] observed a carrier-to-noise ratio of 53 dB and 80 channel television transmission was demonstrated using packaged polymer modulators. A similar demonstration was effected by researchers at IBM. Researchers at TACAN also investigated long term drive voltage stability, DC bias voltage stability, and optical power handling capability. Polymeric modulators exhibited good V_π voltage stability; no detectable change was observed over a period of a year in a typical long term performance test. This result is not surprising when correlated with studies (including at elevated temperatures) noted earlier that report greater than 95% retention of electro-optic activity after 4 years. Polymeric modulators exhibited very little bias voltage drift (less than 10% drift over a 120 h period). Moreover, no runaway behavior (i.e. a continuous drift in one direction) was observed.

Photochemical stability is more difficult to discuss. Two mechanisms have been identified to account for the instability of some electro-optic modulators at power levels. The first mechanism is reorientation of chromophores (for example, azobenzenes) by photo-induced isomerization. The second mechanism involves photo-sensitized oxidation of chromophores. Results vary as expected from chromophore to chromophore and with the nature of the polymer lattice (i.e. the degree of lattice hardening that has been carried out). TACAN has evaluated photochemical stability for various azobenzene chromophores (PU-DR19[35] and LD-3[32]) over the spectral range 543 to 1320 nm. Except for the anticipated photo-induced depoling at visible wavelengths, no instability was observed for low power (10 mW 1.3 µm light) even with exposure for long periods of time. Long-term exposure to 150 mW 1.3 µm light showed detectable degradation of modulator performance for modulators fabricated from PU-DR19. LD-3 materials exhibited significantly greater stability. The results reported by Shi et al.[55] are consistent with the results shown in Fig. 11.

In summary, polymeric modulators have exhibited significantly greater bandwidths than modulators fabricated from inorganic materials. Drive voltage requirements of polymeric modulators have recently fallen below those of inorganic modulators. The total insertion loss of polymeric electro-optic devices is comparable to that of GaAs modulator devices and approximately twice that of lithium niobate devices. Recent reduction in material and processing-associated optical losses for polymeric modulators, together with improvements in
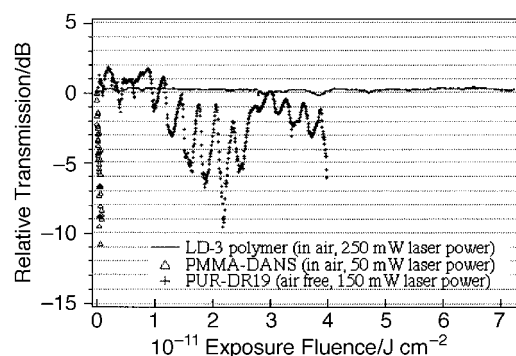

Fig. 11 The relative photostability of three types of polymeric electro-optic materials. The LD-3 material involves a DR chromophore with both ends attached to a PMMA polymer matrix[32] and results for this material are denoted by a solid line. Note that the highest laser power (250 mW) is applied to this material and that no photochemical change is observed to the highest fluence levels. Data denoted by crosses are for a PU-DR19 chromophore attached by one end to a crosslinked polyurethane polymer matrix. The PMMA-DANS material was obtained from IBM-Almaden and consists of an diaminonitrostilbene chromophore attached by one end of the chromophore to an uncrosslinked PMMA polymer. The data support the generally observed result that both thermal and photochemical stability depend strongly upon the hardness of the electro-optic material.

mode matching between passive and active waveguides, suggest that insertion losses for polymeric electro-optic devices may approach those of lithium niobate modulators. The drive and bias voltage stability of polymeric modulators are comparable or superior to those of inorganic modulators. Photochemical stability appears comparable.

Acknowledgements

References

1 B. A. Smith, M. Jurich, W. E. Moerner, W. Volksen, M. E. Best, W. Fleming, J. D. Swalen and G. C. Bjorklund, *Proc. SPIE*, 1993, **2025**, 499; Y. Shi, W. Wang, J. H. Bechtel, A. Chen, S. Garner, S. Kalluri, W. H. Steier, D. Chen, H. R. Fetterman, L. R. Dalton and L. Yu, *IEEE J. Quantum Electron.*, 1966, **2**, 289; J. I. Thackara, G. C. Bjorklund, W. Fleming, M. Jurich, B. A. Smith and J. D. Swalen, *Proc. SPIE*, 1993, **2025**, 564; J. I. Thackara, J. C. Chon, G. C. Bjorklund, W. Volksen and D. M. Burland, *Appl. Phys. Lett.*, 1995, **67**, 3874; L. Dalton, A. Harper, A. Ren, F. Wang, G. Todorova, J. Chen, C. Zhang and M. Lee, *Ind. Eng. Chem. Res.*, 1999, **35**, 8; R. A. Norwood, R. Blomquist, L. Eldada, C. Glass, C. Poga, L. W. Shacklette, B. Xu, S. Yin and J. T. Yardley, *Proc. SPIE*, 1998, **3281**, 2; Y. Shi, W. Wang, J. H. Bechtel, A. Chen, S. Garner, S. Kalluri, W. H. Steier, D. Chen, H. R. Fetterman, L. R. Dalton and L. Yu, *IEEE J. Sel. Top. Quantum Electron.*, 1996, **2**, 289; S. E. Miller and I. P. Kaminow, *Optical Fiber Telecommunications II*, Academic Press, New York, 1988.

2 R. Wiesmann, S. Kalveram, S. Rudolph, M. Johnck and A. Neyer, *Electron. Lett.*, 1996, **32**, 2329; Y. S. Liu, R. J. Wojnarowski, W. A. Hennessy, P. A. Piacente, J. Rowlette, M. Kadar-Kallen, J. Stack, Y. Liu, A. Peczalski and A. Nahata, *Proc. SPIE*, 1988, **3288**, 60; T. Sakano, T. Matsumoto and K. Noguchi, *Appl. Opt.*, 1995, **34**, 1815; L. Eldada, A. Nahata and J. T. Yardley, *Proc. SPIE*, 1998, **3288**, 175; L. J. Camp, R. Sharma and M. R. Feldman, *Appl. Opt.*, 1994, **33**, 6168; J. Gan, B. Bihari, L. Wu, F. Li, M. Dubinovsky, R. T. Chen and S. Tang, *Proc. SPIE*, 1998, **3288**, 122.

3 P. R. Ashley and J. S. Cites, *Opt. Soc. Am. Technol. Digest Ser.*, 1997, **14**, 196.

4 L. R. Dalton, *Kirk-Othmer Encyclopedia of Chemical Technology*, Wiley, New York, 4th edn., 1996, vol. 17, p. 287; L. R. Dalton,

A. W. Harper, B. Wu, R. Ghosn, J. Laquinadanum, Z. Liang, A. Hubbel and C. Xu, *Adv. Mater.*, 1995, **7**, 519; L. R. Dalton, A. W. Harper, R. Ghosn, W. H. Steier, M. Ziari, H. R. Fetterman, Y. Shi, R. V. Mustacich, A. K. Y. Jen and K. J. Shea, *Chem. Mater.*, 1995, **7**, 1060.

5 D. Chen, D. Bhattacharya, A. Udupa, B. Tsap, H. R. Fetterman, A. Chen, S. S. Lee, J. Chen, W. H. Steier and L. R. Dalton, *IEEE Photonics Technol. Lett.*, 1999, **11**, 54; D. Chen, H. R. Fetterman, A. Chen, W. H. Steier, L. R. Dalton, W. Wang and Y. Shi, *Appl. Phys. Lett.*, 1997, **70**, 3335; *Proc. SPIE*, 1997, **3006**, 314; L. R. Dalton and A. W. Harper, *Polym. News*, 1998, **23**, 114; L. Dalton, A. Harper, A. Ren, F. Wang, G. Todorova, J. Chen, C. Zhang and M. Lee, *Ind. Eng. Chem. Res.*, 1999, **35**, 8; H. R. Fetteman, *Proc. RF Photonics: Materials and Devices*, University of California, Los Angeles, 22 October, 1998.

6 S. Kalluri, Z. Ziari, A. Chen, V. Chuyanov, W. H. Steier, D. Chen, B. Jalali, H. Fetterman and L. R. Dalton, *IEEE Photonics Technol. Lett.*, 1996, **8**, 644; S. Kalluri, A. Chen, M. Ziari, W. H. Steier, Z. Liang, L. R. Dalton, D. Chen, B. Jalali and H. R. Fetterman, *Opt. Soc. Am. Technol. Digest Ser.*, 1995, **21**, 317; S. Kalluri, A. Chen, V. Chuyanov, M. Ziari, W. H. Steier and L. R. Dalton, *Proc. SPIE*, 1995, **2527**, 375; L. Dalton, A. Harper, A. Ren, F. Wang, G. Todorova, J. Chen, C. Zhang and M. Lee, *Ind. Eng. Chem. Res.*, 1999, **35**, 8; S. Kalluri, Ph.D. Thesis, University of Southern California, 1997; W. H. Steier, A. Chen, S. S. Lee, S. Garner, H. Zhang, V. Chuyanov, L. R. Dalton, F. Wang, A. S. Ren, C. Zhang, G. Todorova, A. Harper, H. R. Fetterman, D. Chen, A. Udupa, D. Bhattacharya and B. Tsap, *Chem. Phys.*, in the press; S. M. Garner, V. Chuyanov, S. S. Lee, A. Yacoubian, A. Chen, W. H. Steier, F. Wang, A. S. Ren, M. He and L. R. Dalton, *IEEE Photonics Technol. Lett.*, 1999, **11**, 842.

7 P. N. Prasad and D. J. Williams, *Introduction to Nonlinear Optical Effects in Molecules and Polymers*, Wiley, New York, 1991; G. A. Lindsay and K. D. Singer, *Polymers for Second-order Nonlinear Optics*, American Chemical Society, Washington, D. C., 1995; D. J. Williams, *Nonlinear Optical Properties of Organic and Polymeric Materials*, American Chemical Society, Washington, D. C., 1983; D. S. Chemla and J. Zyss, *Nonlinear Optical Properties of Organic Molecules and Crystals*, Academic Press, New York, 1987; C. Bosshard, K. Sutter, P. Pretre, J. Hulliger, M. Florsheimer, P. Kaatz and P. Gunter, *Organic Nonlinear Optical Materials*, Gordon and Breach, New York, 1995; R. W. Boyd, *Nonlinear Optics*, Academic Press, New York, 1992; Y. R. Shen, *The Principles of Nonlinear Optics*, Wiley, New York, 1984; P. N. Butcher and D. Cotter, *The Elements of Nonlinear Optics*, Cambridge University Press, New York, 1990; A. Yariv and P. Yeh, *Optical Waves in Crystals*, Wiley, New York, 1984; H. S. Nalwa and S. Miyata, *Nonlinear Optics of Organic Molecules and Polymers*, CRC Press, Boca Raton, FL, 1997; D. L. Wise, G. E. Wnek, D. J. Trantolo, T. M. Cooper and J. D. Gresser, *Electrical and Optical Polymer Systems*, Marcel Dekker, New York, 1998; J. Zyss and J. L. Oudar, *Phys. Rev. A*, 1982, **26**, 2028; K. D. Singer, M. G. Kuzyk and J. E. Sohn, *J. Opt. Soc. Am.*, 1987, **4**, 968; H. E. Katz, K. D. Singer, J. E. Sohn, C. W. Dirk, L. A. King and H. E. Gordon, *J. Am. Chem. Soc.*, 1987, **109**, 6561; J. L. Oudar, D. S. Chemla and E. Batifol, *J. Chem. Phys.*, 1977, **66**, 2664; D. A. Kleinman, *Phys. Rev.*, 1962, **126**, 1977; W. Ren, S. Bauer, S. Yilmaz, W. Wirges and R. Gerhard-Multhaupt, *Appl. Phys. Lett.*, 1994, **65**, 7211; R. A. Hill, A. Knoesen and M. A. Mortazavi, *Appl. Phys. Lett.*, 1994, **65**, 1733; C. P. J. M. v. d. Vorst and S. J. Picken, *J. Opt. Soc. Am. B*, 1990, **7**, 320; M. G. Kuzyk, J. E. Sohn, and C. W. Dirk, *J. Opt. Soc. Am. B*, 1990, **7**, 842.

8 S. R. Marder, D. N. Beratan and L. T. Cheng, *Science*, 1991, **252**, 103; C. B. Gorman and S. R. Marder, *Proc. Natl. Acad. Sci. USA*, 1993; **90**, 11297; S. R. Marder and J. W. Perry, *Science*, 1994, **263**, 1706; G. Boruhill, L. T. Cheng, G. Lee, S. R. Marder, J. W. Perry, M. J. Perry and B. G. Tiemann, *Mater. Res. Soc. Symp. Proc.*, 1994, **328**, 625; S. B. Marder, C. B. Gorman, F. Meyers, J. W. Perry, G. Bourhill, J. L. Bredas and B. M. Pierce, *Science*, 1994, **265**, 632; A. K. Y. Jen, Y. Cai, P. V. Bedworth and S. R. Marder, *Adv. Mater.*, 1997, **9**, 132; H. E. Katz, K. D. Singer, J. E. Sohn, C. W. Dirk, L. A. King and H. E. Gordon, *J. Am. Chem. Soc.*, 1987, **109**, 6561.

9 A. W. Harper, Ph.D. Thesis, University of Southern California, 1997.

10 D. R. Kanis, M. A. Ratner and T. J. Marks, *Chem. Rev.*, 1994, **94**, 195; A. F. Garito, K. Y. Wong, Y. M. Cai, H. T. Man and O. Zamani-Khamiri, *Proc. SPIE*, 1986, **682**, 2; J. R. Heflin, K. Y. Wong, O. Zamani-Kharmiri and A. F. Garito, *Phys. Rev. B*, 1988, **38**, 1573.

11 D. M. Burland, R. D. Miller and C. A. Walsh, *Chem. Rev.*, 1994, **94**, 31; C. R. Moylan, R. J. Twieg, V. Y. Lee, S. A. Swanson, K. M. Betterton and R. D. Miller, *J. Am. Chem. Soc.*, 1993, **115**, 12599; S. Ermer, S. M. Lovejoy, D. S. Leung, H. Warren, C. R. Moyland and R. J. Twieg, *Chem. Mater.*, 1997, **9**, 1498; Y. Zhang, A. K. Y. Jen, T. Chen, Y. Liu, X. Zhang and J. T. Kenney, *Proc. SPIE*, 1997, **3006**, 372; A. K. Y. Jen, X. M. Wu and H. Ma, *Chem. Mater.*, 1998, **10**, 471; H. Ma, X. Wang, X. Wu, S. Liu and A. K. Y. Jen, *Macromolecules*, 1998, **31**, 4049; L. R. Dalton, A. W. Harper, R. Ghosn, W. H. Steier, M. Ziari, H. Fetterman, Y. Shi, R. V. Mustacich, A. K. Y. Jen and K. J. Shea, *Chem. Mater.*, 1995, **7**, 1060; L. Dalton, A. Harper, A. Ren, F. Wang, G. Todorova, J. Chen, C. Zhang and M. Lee, *Ind. Eng. Chem. Res.*, 1999, **35**, 8; F. Wang, Ph.D. Thesis, University of Southern California, 1998; J. Chen, Ph.D. Thesis, University of Southern California, 1998; C. Zhang, Ph.D. Thesis, University of Southern California, 1999.

12 L. T. Chang, W. Tam, S. R. Marder, A. E. Stiegman, G. Rikken and C. W. Spangler, *J. Phys. Chem.*, 1991, **95**, 10643.

13 K. Clays and A. Persoons, *Phys. Rev. Lett.*, 1991, **66**, 2980.

14 M. Lequan, R. M. Lequan, K. C. Ching, M. Barzoukas, A. Fort, H. Lahoucine, G. Bravic, D.Chasseau and J. Gaultier, *J. Mater. Chem.*, 1992, **2**, 719; K. D. Singer, M. G. Kuzyk and J. E. Sohn, *J. Opt. Soc. Am. B*, 1987, **4**, 968; J. L. Oudar, D. S. Chemla and E. Batifol, *J. Chem. Phys.*, 1977, **66**, 2664; Y. Shi, Ph.D. Thesis, University of Southern California, 1993.

15 C. C. Teng and H. T. Man, *Appl. Phys. Lett.*, 1990, **56**, 1734; Y. Levy, M. Dumont, E. Chastaing, P. Robin, P. A. Chaollet, G. Gadret and F. Kajzar, *Mol. Cryst. Liq. Cryst. Sci. Technol. B*, 1993, **4**, 1.

16 V. Dentan, Y. Levy, M. Dumont, P. Robin and E. Chastaing, *Opt. Commun.*, 1989, **69**, 379.

17 M. Ziari, S. Kalluri, S. Garner, W. H. Steier, Z. Liang, L. R. Dalton and Y. Shi, *Proc. SPIE*, 1995, **2527**, 218; S. Kalluri, S. Garner, M. Ziari, W. H. Steier, Y. Shi and L. R. Dalton, *Appl. Phys. Lett.*, 1996, **69**, 275.

18 M. W. Becker, L. S. Sapochak, R. Ghosn, C. Xu, L. R. Dalton, Y. Shi, W. H. Steier and A. K. Y. Jen, *Chem. Mater.*, 1994, **6**, 104.

19 A. Chen, V. Chuyanov, S. Garner, W. H. Steier and L. R. Dalton, *Opt. Soc. Am. Technol. Digest Ser.*, 1997, **14**, 158.

20 D. M. Burland, R. D. Miller and C. A. Walsh, *Chem. Rev.*, 1994, **94**, 31; T. J. Marks and M. Ratner, *Angew. Chem.*, *Int. Ed. Engl.*, 1995, **34**, 155; L. R. Dalton, A. W. Harper, R. Ghosn, W. H. Steier, M. Ziari, H. Fetterman, Y. Shi, R. V. Mustacich, A. K. Y. Jen and K. J. Shea, *Chem. Mater.*, 1995, **7**, 1060; L. Dalton, A. Harper, A. Ren, F. Wang, G. Todorova, J. Chen, C. Zhang and M. Lee, *Ind. Eng. Chem. Res.*, 1999, **38**, 8; L. R. Dalton, C. Xu, B. Wu and A. W. Harper, in *Frontiers of Polymer Research*, eds. P. N. Prasad and J. Nigam, Plenum, New York, 1993, p. 175.

21 J. P. Bromberg, *Physical Chemistry*, Allyn and Bacon, Newton, MA, 1984, p.851; D. Chandler, *Introduction to Statistical Mechanics*, Oxford, New York, 1987.

22 L. Onsager, *J. Am. Chem. Soc.*, 1936, **58**, 1486.

23 L. R. Dalton, A. W. Harper and B. H. Robinson, *Proc. Natl. Acad. Sci. USA*, 1997, **94**, 4842; L. R. Dalton, A. W. Harper, J. Chen, S. Sun, S. Mao, S. Garner, A. Chen and W. H. Steier, *Proc. SPIE*, 1997, **CR68**, 313; A. W. Harper, S. Sun, L. R. Dalton, S. M. Garner, A. Chen, S. Kalluri, W. H. Steier and B. H. Robinson, *J. Opt. Soc. Am. B*, 1998, **15**, 329; L. Dalton, A. Harper, A. Ren, F. Wang, G. Todorova, J. Chen, C. Zhang and M. Lee, *Ind. Eng. Chem. Res.*, 1999, **35**, 8; B. H. Robinson, L. R. Dalton, A. W. Harper, A. Ren, F. Wang, C. Zhang, G. Todorova, M. Lee, R. Aniszfeld, S. M. Garner, A. Chen, W. H. Steier, S. Houbrecht, A. Persoons, I. Ledoux, J. Zyss and A. K. Y. Jen, *Chem. Phys.*, in the press; J. Chen, Ph.D. Thesis, University of Southern California, 1998; A. W. Harper, Ph.D. Thesis, University of Southern California, 1997; J. Zhu, Ph.D. Thesis, University of Southern California, 1997; S. S. Sun, Ph.D. Thesis, University of Southern California, 1996; A. Piekara, *Proc. R. Soc. London A*, 1939, **149**, 360.

24 F. London, *Trans. Faraday Soc.*, 1937, **33**, 8.

25 H. E. Katz, M. L. Schilling and G. E. Washington, *J. Opt. Soc. Am. B*, 1990, **7**, 309.

26 A. Chen, Ph.D. Thesis, University of Southern California, 1998.

27 F. Wang, Ph.D. Thesis, University of Southern California, 1998.

28 C. Zhang, Ph.D. Thesis, University of Southern California, 1999.

29 S. Ermer, personal communication.

30 L. Dalton, A. Harper, A. Ren, F. Wang, G. Todorova, J. Chen, C. Zhang and M. Lee, *Ind. Eng. Chem. Res.*, 1999, **38**, 8; L. R. Dalton, in *Electrical and Optical Polymer Systems*, eds. D. L. Wise, G. E. Wnek, D. J. Trantolo, T. M. Cooper and J. D. Gresser, Marcel Dekker, New York, 1998, p. 609.

31 Z. Liang, L. R. Dalton, S. M. Garner, S. Kalluri, A. Chen and W. H. Steier, *Chem. Mater.*, 1995, **7**, 941, 1756; Z. Liang, Z. Yang, S. Sun, B. Wu, L. R. Dalton, S. M. Garner, S. Kalluri, A. Chen and W. H. Steier, *Chem. Mater.*, 1996, **8**, 2681; L. R. Dalton, A. W. Harper, R. Ghosn, W. H. Steier, M. Ziari, H. Fetterman, Y. Shi, R. V. Mustacich, A. K. Y. Jen and K. J. Shea, *Chem. Mater.*, 1995, **7**, 1060; K. D. Singer, T. C. Kowalczyk, H. D. Nguyen, A. J. Beuhler and D. A. Wargowski, *Proc. SPIE*, 1997, **CR68**, 399; K. D. Singer, T. C. Kowalczyk, H. D. Nguyen, A. J. Beuhler and D. A. Wargowski, *Proc. SPIE*, 1997, **3006**, 326; M. W. Becker, L. S. Sapochak, L. R. Dalton, Y. Shi, W. H. Steier and Y. Shi, *Chem. Mater.*, 1994, **6**, 104; A. K. Y. Jen, K. J. Drost, Y. Cai, V. P. Rao and L. R. Dalton, *J. Chem. Soc., Chem. Commun.*, 1994, 965.
32 C. Xu, B. Wu, O. Todorova, L. R. Dalton, Y. Shi, P. M. Ranon and W. H. Steier, *Macromolecules*, 1993, **26**, 5303; Y. Shi, P. M. Ranon, W. H. Steier, C. Xu, B. Wu and L. R. Dalton, *Appl. Phys. Lett.*, 1993, **63**, 2168; W. H. Steier, Y. Shi, P. M. Ranon, C. Xu, B. Wu, L. R. Dalton, W. Wang, D. Chen and H. R. Fetterman, *Proc. SPIE*, 1993, **2025**, 546; Y. Shi, P. M. Ranon, W. H. Steier, C. Xu, B. Wu and L. R. Dalton, *Proc. SPIE*, 1993, **2025**, 106; C. Xu, B. Wu, L. R. Dalton, Y. Shi, P. M. Ranon and W. H. Steier, *Macromolecules*, 1992, **25**, 6714; D. M. Burland, R. D. Miller and C. A. Walsh, *Chem. Rev.*, 1994, **94**, 31; T. J. Marks and M. Ratner, *Angew. Chem., Int. Ed. Engl.*, 1995, **34**, 155; L. R. Dalton, A. W. Harper, R. Ghosn, W. H. Steier, M. Ziari, H. Fetterman, Y. Shi, R. V. Mustacich, A. K. Y. Jen and K. J. Shea, *Chem. Mater.*, 1995, **7**, 1060.
33 B. Wu, C. Xu, L. R. Dalton, S. Kalluri, Y. Shi and W. H. Steier, *Mater. Res. Soc. Symp. Proc.*, 1994, **328**, 529; C. Xu, B. Wu, M. W. Becker, L. R. Dalton, P. M. Ranon, Y. Shi and W. H. Steier, *Chem. Mater.*, 1993, **5**, 1439; P. M. Ranon, Y. Shi, W. H. Steier, C. Xu, B. Wu and L. R. Dalton, *Appl. Phys. Lett.*, 1993, **62**, 2605; C. Xu, B. Wu, L. R. Dalton, Y. Shi, P. M. Ranon and W. H. Steier, *Macromolecules*, 1992, **25**, 6716.
34 H. W. Oviatt, Jr., K. J. Shea, S. Kalluri, Y. Shi, W. H. Steier and L. R. Dalton, *Chem. Mater.*, 1995, **7**, 493; S. Kalluri, Y. Shi, W. H. Steier, Z. Yang, C. Xu and L. R. Dalton, *Appl. Phys. Lett.*, 1994, **65**, 2651; S. Kalluri, W. H. Steier, Z. Yang, C. Xu, B. Wu, L. R. Dalton, Y. Shi and J. H. Bechtel, *Proc. SPIE*, 1994, **2285**, 67; Z. Yang, C. Xu, B. Wu, L. R. Dalton, S. Kalluri, W. H. Steier, Y. Shi and J. H. Bechtel, *Chem. Mater.*, 1994, **6**, 1899; J. B. Caldwell, R. W. Cruse, K. J. Drost, V. P. Rao, A. K. Y. Jen, K. Y. Wong, Y. M. Cai, R. M. Mininni, J. Kenny, E. Binkley, L. R. Dalton, Y. Shi and W. H. Steier, *Mater. Res. Soc. Symp. Proc.*, 1994, **328**, 535.
35 M. Chen, L. P. Yu, L. R. Dalton, Y. Shi and W. H. Steier, *Macromolecules*, 1991, **24**, 5421; M. Chen, L. R. Dalton, L. P. Yu, Y. Shi and W. H. Steier, *Macromolecules*, 1992, **25**, 4032; Y. Shi, W. H. Steier, M. Chen, L. P. Yu and L. R. Dalton, *Appl. Phys. Lett.*, 1992, **1775**, 379.
36 S. S. H. Mao, Y. Ra, L. Guo, C. Zhang, L. R. Dalton, A. Chen, S. Garner and W. H. Steier, *Chem. Mater.*, 1998, **10**, 146; Y. Ra, Ph.D. Thesis, University of Southern California, 1997.
37 C. C. Teng, *Appl. Opt.*, 1993, **32**, 1051; C. C. Teng, M. A. Mortazavi and G. K. Boudoughian, *Appl. Phys. Lett.*, 1995, **66**, 667; A. Chen, Ph.D. Thesis, University of Southern California, 1998.
38 W. H. Steier, S. Kalluri, A. Chen, S. Garner, V. Chuyanov, M. Ziari, Y. Shi, H. Fetterman, B. Jalali, W. Wang, D. Chen and L. R. Dalton, *Mater. Res. Soc. Symp. Proc.*, 1996, **413**, 147; A. Chen, K. Kaviani, A. Remple, S. Kalluri, W. H. Steier, Y. Shi, Z. Liang and L. R. Dalton, *J. Electrochem. Soc.*, 1996, **143**, 3648.
39 S. M. Garner, Ph.D. Thesis, University of Southern California, 1998; S. Garner, V. Chuyanov, A. Chen, S. S. Lee, W. H. Steier and L. R. Dalton, *Proc. SPIE*, 1998, **3278**, 259; S. M. Garner, V. Chuyanov, S. S. Lee, A. Chen, W. H. Steier and L. R. Dalton, *IEEE Photonics Technol. Lett.*, 1999, **11**, 842; W. H. Steier, A. Chen, S. S. Lee, S. Garner, H. Zhang, V. Chuyanov, L. R. Dalton, F. Wang, A. S. Ren, C. Zhang, G. Todorova, A. Harper, H. R. Fetterman, D. Chen, A. Udupa, D. Bhattacharya and B. Tsap, *Chem. Phys.*, in the press.
40 R. Yoshimura, M. Hikita, S. Tomaru and S. Imamura, *IEEE J. Lightwave Technol.*, 1998, **16**, 1030; Y. Koike, T. Ishigure and E. Nihei, *IEEE J. Lightwave Technol.*, 1995, **13**, 1475.
41 T. Watanabe, M. Hikita, M. Amano, Y. Shuto and S. Tomaru, *J. Appl. Phys.*, 1998, **83**, 639.
42 A. Chen, V. Chuyanov, F. I. Marti-Carrera, S. Garner, W. H. Steier, J. Chen, S. Sun and L. R. Dalton, *Proc. SPIE*, 1997, **3005**, 65; L. Dalton, A. Harper, A. Ren, F. Wang, G. Todorova, J. Chen, C. Zhang and M. Lee, *Ind. Eng. Chem. Res.*, 1999, **38**, 8; A. Chen, Ph.D. Thesis, University of Southern California, 1998; S. Kalluri, Ph.D. Thesis, University of Southern California, 1997.
43 S. Garner, V. Chuyanov, A. Chen, S. S. Lee, W. H. Steier and L. R. Dalton, *Proc. SPIE*, 1998, **3278**, 259; S. Garner, V. Chuyanov, A. Chen, A. Yacoubian, W. H. Steier and L. R. Dalton, *Proc. IEEE/LEOS*, 1997, **1**, 264; S. M. Garner, Ph.D. Thesis, University of Southern California, 1998.
44 S. M. Garner, S. S. Lee, V. Chuyanov, A. Yacoubian, A. Chen, W. H. Steier, J. Zhu, J. Chen and L. R. Dalton, ICAPT'98, Ottawa, Canada; S. M. Garner, Ph.D. Thesis, University of Southern California, 1998.
45 X. F. Cao, L. P. Yu and L. R. Dalton, *Opt. Soc. Am. Technol. Digest Ser.*, 1990, 165; L. R. Dalton, L. S. Sapochak, M. Chen and L. P. Yu, in *Molecular Electronics and Molecular Electronic Devices*, vol. 2, ed. K. Sienicki, CRC Press, Boca Raton, FL, 1993, p. 125; X. L. Jiang, L. Li, J. Kumar and S. K. Tripathy, *Appl. Phys. Lett.*, 1996, **69**, 3629.
46 W. H. Steier, A. Chen, S. S. Lee, S. Garner, H. Zhang, V. Chuyanov, L. R. Dalton, F. Wang, A. S. Ren, C. Zhang, G. Todorova, A. Harper, H. R. Fetterman, D. Chen, A. Udupa, D. Bhattacharya and B. Tsap, *Chem. Phys.*, in the press.
47 Y. Shi, W. H. Steier, L. Yu, M. Chen and L. R. Dalton, *Appl. Phys. Lett.*, 1991, **59**, 2935; Z. Sekkat, J. Wood, E. F. Aust, W. Knoll, W. Volksen and R. D. Miller, *J. Opt. Soc. Am. B*, 1996, **13**, 1713.
48 J. H. Bechtel and Y. Shi, *Proc. RF Photonics: Materials and Devices*, University of California, Los Angeles, 22nd October, 98.
49 D. Chen, D. Bhattacharya, A. Udupa, B. Tsap, H. R. Fetterman, A. Chen, S. S. Lee, J. Chen, W. H. Steier and L. R. Dalton, *IEEE Photonics Technol. Lett.*, 1999, **11**, 54.
50 W. Wang, Y. Shi, D. J. Olson, W. Lin and J. H. Bechtel, *IEEE Photonics Technol. Lett.*, 1999, **11**, 51.
51 G. L. Abbas, V. W. S. Chan and T. K. Yee, *IEEE J. Lightwave Technol.*, 1985, **3**, 1110.
52 A. Chen, V. Chuyanov, F. I. Marti-Carrera, S. Garner, W. H. Steier, S. S. H. Mao, Y. Ra and L. R. Dalton, *IEEE Photonic Technol. Lett.*, 1997, **9**, 1499; A. Chen, V. Chuyanov, F. I. Marti-Carrera, S. Garner, W. H. Steier and L. R. Dalton, *Proc. SPIE*, 1997, **3147**, 268.
53 J. F. Coward, T. K. Yee, C. H. Chalfant and P. H. Chang, *IEEE J. Lightwave Technol.*, 1993, **11**, 2201.
54 A. Chen, V. Chuyanov, H. Zhang, S. Garner, W. H. Steier, J. Chen, J. Zhu, M. He, S. S. H. Mao and L. R. Dalton, *Opt. Lett.*, 1998, **23**, 478; A. Chen, V. Chuyanov, H. Zhang, S. Garner, S. S. Lee, W. H. Steier, J. Chen, F. Wang, J. Zhu, M. He, Y. Ra, S. S. H. Mao, A. W. Harper, L. R. Dalton and H. R. Fetterman, *Proc. SPIE*, 1998, **3281**, in the press.
55 Y. Shi, W. Wang, J. H. Bechtel, A. Chen, S. Garner, S. Kalluri, W. H. Steier, D. Chen, H. R. Fetterman, L. R. Dalton and L. Yu, *IEEE J. Quantum Electron.*, 1966, **2**, 289.

Paper 9/02659B